research review

OFFICE of AEROSPACE RESEARCH

OAR: The Research Agency
of The United States Air Force

VOLUME VI NUMBER 5 MAY 1967

Algebraic Methods in Particle Physics

PROFESSOR YUVAL NE'EMAN, Physics Department, Tel-Aviv University, Israel

Quantum mechanics is basically an algebraic theory. It deals with observables whose description is given by linear Hermitean operators acting on a Hilbert space. The more sophisticated concept of a quantized field is an extension, apparently suitable for the treatment of quantum electrodynamical effects such as anomalous magnetic moments (for electrons and muons), the Lamb shift in hydrogen, various radiative corrections, etc. Axiomatic field theorists now study the algebraic structure of such quantized fields. It is remarkable that this should still be a mystery, even though the theory supplied all the observationally correct answers between 1946 and 1950.

To describe strong and weak interactions, a third algebraic layer is being added at present. Before reviewing this subject, let us first trace the developments which have led up to it.

The model provided by quantum electrodynamics seems appropriate as far as most* weak interactions are concerned. It has been known since 1958 that the law of the weak force can be formulated as a product of two currents $H = \sum_{\mu=0,1,2,3} j_W^\mu (j_W^\dagger)^\mu$ + Hermitean conjugate. Thus, the static component of the force is given by the product of two "weak" charges j_W^0, just as in the Coulomb law. The weak current j_W^μ is an ordinary vector quantity v_W^μ (like the electric current) 50% of the time. The other 50% of the weak current forms an "axial" vector a_W^μ whose space components $a_W^{1,2,3}$ do not change sign under spatial reflection, whereas the sign of the time component (the axial charge a_W^0) is inverted. It is the interference term in the product of the two charges which violates parity, since the vector charge v_W^0 is a true scalar.

The weak charge is "universal" in the sense that it is the same for different particles, just as the electric charges of the proton and electron have the same magnitude. This is mostly true of the charge v_W^0 carried by the vector current, a conserved quantity satisfying an equation of continuity $\sum_\mu \frac{\partial}{\partial x^\mu} v^\mu = 0$.

The axial-vector current a^μ is not conserved, and there is thus no necessity that its charge should be universal. It turns out, however,

*It is not clear whether this applies to the non-leptonic part of the weak interactions.

AIR FORCE OFFICE of SCIENTIFIC RESEARCH ★ The FRANK J. SEILER RESEARCH LABORATORY
AIR FORCE CAMBRIDGE RESEARCH LABORATORIES ★ AEROSPACE RESEARCH LABORATORIES
OFFICE of RESEARCH ANALYSES ★ EUROPEAN OFFICE, OAR ★ LATIN AMERICAN OFFICE, OAR

that this $\sum_{\mu} \frac{\partial}{\partial x^{\mu}} a^{\mu} \neq 0$ "leakage" causes a difference of some 20% only in the strength of the coupling; in other words, the axial charge $|G_A| \simeq 1.2\ G_V$, G_V being the conserved vector charge (similar to e, the electron charge in electrodynamics), proportional to $\int dV\ v_W^o$.

Let us now turn to the strong interactions. These do not fit a description in terms of quantized fields. The physical identification of a current requires it to be coupled "weakly" to an external field. With the electric coupling $\frac{e^2}{4\pi} = \frac{1}{137}$, we can safely use a perturbation expansion and measure electromagnetic transitions corresponding to the exchange of one photon γ or to its emission, as in $\Sigma^o \to \Lambda + \gamma$, the main mode of Σ^o decay. These matrix elements make up the electromagnetic current. Similarly, the smallness of G_V^2, G_A^2 or $G_A G_V$ enables us to attribute the entire $n \to p + e^- + \bar{\nu}_e$ transitions of beta decay to the first-order coupling between the $(\bar{p}n)$ hadron* current and the $(\bar{e}\nu_e)$ lepton current. Such a factorization does not exist in the field description of the strong interaction. We can compare the "strong" decay $\Delta^{++} \to p + \pi^+$ (Δ is the nucleon-pion resonance at 1,238 MeV, spin (J) and parity (P) $J^P = \frac{3^+}{2}$ and isospin $I = \frac{3}{2}$), with the electromagnetic decay $\Sigma^o \to \Lambda + \gamma$. A higher-order electromagnetic radiative correction such as the emission and reabsorption of an addi-

Hadron, a strongly interacting particle. The $\bar{p}$ implies creation of a proton (or annihilation of an antiproton); the n implies annihilation of a neutron (or creation of an antineutron).

research review
OFFICE OF AEROSPACE RESEARCH

OAR RESEARCH REVIEW is published monthly by the Office of Scientific and Technical Information (RRYC), Hq Office of Aerospace Research, USAF, 1400 Wilson Boulevard, Arlington, Va. 22209. The objective of this publication is to make a positive contribution to the exchange of information concerning Air Force conducted and sponsored research activities.

JACOB SEIDEN Editor

ALGEBRAIC METHODS IN PARTICLE PHYSICS
Professor Yuval Ne'eman 1

CLOUD ROWS OVER FLORIDA
Meteorology Laboratory, AFCRL 7

ORGANOSULFUR INTERMEDIATES
Dr. Anthony J. Matuszko 9

ALBEDO CONTRIBUTIONS TO THE IONOSPHERE
Upper Atmosphere Physics Laboratory, AFCRL 10

MAGNETIC FIELD GEOMETRICS IN A TANK
Space Physics Laboratory, AFCRL 12

CONFERENCE ON INTELLIGENT SYSTEMS
Rowena Swanson 14

A CONTROL–SYSTEMS STUDY OF THE HUMAN EYE–POSITIONING MECHANISM
1st Lt Gerald Cook 15

A METHOD OF DETERMINING ANGULAR MOMENTA OF NUCLEAR EXCITED STATES
1st Lt Henry Willmes 16

THERMOELECTRIC POWER AND ELECTRICAL CONDUCTIVITY OF NbO_2
James A. Roberson 20

SPHERICAL–IMPLOSION LAUNCHING TECHNIQUES
John W. Goresh 24

HEXAGONAL DIAMOND—A NEW FORM OF CARBON
Dr. William L. Ruigh 26

BALLOON TRAJECTORY CONTROL AND PREDICTION
Aerospace Instrumentation Laboratory, AFCRL 27

ATLAS ON ATMOSPHERIC HUMIDITY IN NORTHERN HEMISPHERE PUBLISHED
Aerospace Instrumentation Laboratory, AFCRL 29

PREDICTION OF SHOCK SHAPES
Major John P. Thomas 32

DISTRIBUTION OF THIS DOCUMENT IS UNLIMITED

For sale by the Superintendent of Documents, U.S. Government Printing Office Washington, D.C. 20402 - $2.75 per year domestic, 75 cents additional for foreign mailing, 25 cents per single copy and 15 cents per Annual Index. Back issues will not be furnished.

tional photon involves an additional factor of $\frac{1}{137}$ in the amplitude (or 10^{-4} in the cross section) and can thus be safely disregarded. The same cannot be said for the strong processes where, for instance, $\Delta^{++} \rightarrow p + \pi^+ + \pi^0 \rightarrow p + \pi^+$ could be more important than the original reaction, since $g^2_{strong}/4\pi \sim 15$.

To cope with this problem, strong interaction theorists were led to develop non-perturbative methods. The most successful method consists in Dispersion Relations. These are based upon a study of the analytical structure of the S-matrix amplitudes. Field theory is sometimes used, but just as a clue to the mechanism responsible for the appearance of poles or cuts in the complex energy plane. In that sense it turns out, for instance, that one of the main mechanisms contributing to the above Δ^{++} decay (or its reversed $p + \pi^+ \rightarrow \Delta^{++}$) is the exchange reaction $p + \pi^+ \rightarrow (\pi^+ + n) + \pi^+ \rightarrow \pi^+ + (n + \pi^+) \rightarrow \pi^+ + p$, with the Δ^{++} representing a resonance of the $p + \pi^+$ elastic scattering amplitude. In this process, the neutron appears as a pole at $(939\ MeV)^2$ in the complex plane of the analytically continued momentum-transfer squared (since the neutron is crossing over to the pion's position).

Another advance in these analytical methods came in 1959 with analytical continuation in angular momentum J. Drawing from non-relativistic quantum mechanics, it was conjectured that high-energy scattering could be described in terms of "mediation" by a "Regge trajectory." A trajectory in the complex J plane represents a continuous set of solutions to a Schrödinger-like equation, with the actual physical particles it relates appearing as poles at integer J along the trajectories. The 1s, 2p, 3d, etc. states in hydrogen, for instance, make up such a trajectory. It turned out that, under certain conditions, an amplitude could be factorized into two current-like vertices connected by such a trajectory. For instance, the $\pi^+ + n \rightarrow \pi^0 + p$ charge-exchange scattering should be given beyond some 5-6 BeV/c pion laboratory-energy by the exchange of a trajectory whose lowest pole is the ρ^+ meson with $J^P = 1^-$ at 750 MeV; the next pole appears with $J^P = 3^-$ at about 2 BeV, and so on.

At that stage, an attempt was made to reduce strong interactions to just these dynamics--by the boot-strap assumption. In such a picture, no hadron is regarded as elementary; all hadron states are considered as compounds of other hadron states, and one assumes that the set of self-consistent dynamical equations stating this connection suffices for the calculation of all masses. It should also determine the composition of the hadron spectrum entirely. This approach provided some qualitative insights, but could not yield the required answers. It seems that the description of strong forces involves more than purely kinematical information at this stage.

This is where group theory has provided several of the missing clues. To begin with, it turned out that the strong interactions display an "internal" symmetry--the word, "internal," implying that this symmetry is not a space-time feature. One part of this symmetry, known as charge independence, had already been discovered in the thirties. Breit had then noticed that proton-proton, proton-neutron and neutron-neutron forces appeared to be equal, if one first deducted differences due to electromagnetism. This symmetry could be represented as the rotational invariance of the Hamiltonian in a mathematical representation space (an "isospace") in which the nucleon appeared as N, a 2-component spinor (p, n). The nucleon-pion interaction (or vertex) should be represented by an isospace scalar $(\bar{N}\underline{\tau}N)\cdot\underline{\pi}$, where $\underline{\tau}$ stands for the 3 Pauli 2x2 matrices--also the abstract generators of the algebra of SU(2), or isospin I. The I-spin transformation $\bar{N}\underline{\tau}N$ reproduces the currents $(\bar{p}n)$, $(\bar{n}p)$ and $(\bar{p}p - \bar{n}n)/\sqrt{2}$.

In 1961-64 it became clear that the entire realm of strong interactions, including those of strange particles, displayed an approximate SU(3) symmetry. The isospace had to be enlarged to 8 dimensions (the "Eightfold Way") with charge-independence now being replaced by an approximate "charge and strangeness" independence. Forces (or amplitudes) were invariant under unitary transformations (i.e., co-ordinate transformations

preserving lengths in a complex space) in the enlarged isospace. However, as implied by the notation, SU(3) represented invariance under the most general unitary transformations in a 3-dimensional complex space, not an 8-dimensional one. Out of the 64 linearly independent unitary transformations one can enact in an 8-dimensional space, only 9 particular combinations corresponded to the symmetry of the "Eightfold Way" (8 in fact, plus the identity). In other words, the lowest-lying baryons (the nucleon doublet and six hyperons Λ°, Σ^{+}, Σ°, Σ^{-}, Ξ°, Ξ^{-}) form an 8-dimensional representation of SU(3), i.e., a basis in an 8-dimensional space in which we require invariance under just 8 linearly independent rotations. The simplest model reproducing this result, which H. Goldberg and I put forward in 1962, represents the baryon octet as the direct product (i.e., a "compound") of 3 "basic" objects corresponding to the 3 states of the defining representation of SU(3). Denoting these states as A, B, C, we can represent the proton as (AAB), the neutron as (ABB), and so on. It turns out that A has to have an electric charge of $\frac{2}{3}$ e, B and C have $-\frac{1}{3}$ e (where e is the proton charge); their baryon number is, of course, $\frac{1}{3}$. The question was taken up in 1964 by M. Gell-Mann and G. Zweig, who made the daring suggestion that such states ("quarks" or "aces") might actually exist in nature, quite aside from their role in the mathematical model. The search for quarks has as yet only produced a lower bound on their allowed masses--in other words, if they exist they are not found because of the energy requirements in their production.

Unitary symmetry, based upon the identification of the baryon octet as an SU(3) representation, has been very successful as a classification scheme, as a basis for the derivation of intensity rules and the calculation of magnetic moments, weak-interaction decays, etc.

Unitary symmetry enables us to group the various hadrons into multiplets. To date, these have been octets, decimets and singlets. Four meson octets and singlets (forming together reducible "nonets") are now known, with spins $J^{P} = 0^{-}, 1^{-}, 1^{+}, 2^{+}$. An incomplete 0^{-} multiplet (three π and four K mesons) was the only known set when the theory was first promulgated. It was straightforward to predict the missing eighth 0^{-} component, the η (550 MeV) meson. For the baryons, we have definite identifications for $J = \frac{1}{2}^{+}, \frac{3}{2}^{-}, \frac{5}{2}^{+}$ octets, for $J = \frac{3}{2}^{+}, \frac{7}{2}^{+}$ decimets and for $J = \frac{1}{2}^{-}, \frac{3}{2}^{-}$ singlets. The $J = \frac{3}{2}^{+}$ decimet was "filled-up" with the discovery of the Ω^{-}, whose mass and other quantum numbers were entirely predicted from the theory. Note that in "quark notation" the Ω^{-} is (CCC), a totally symmetric combination in both unitary spin and ordinary spin, since $J = \frac{3}{2}$. This is also true of the entire decimet, and is now known to hold for the baryon octet as well. Quarks, if they really make up the known hadrons, have to have peculiar statistical properties, which make them more improbable.

A symmetry can always be reduced to a conservation law; unitary symmetry being only approximate, we get the approximate conservation of Unitary Spin, an 8-component quantity--or, adjoining baryon number conservation, a 9-component one. The symmetry-breaking effect which generates the mass-differences within a multiplet (938, 1115, 1195 and 1325 MeV for N, Λ, Σ, Ξ in the baryon octet for instance) displays a definite behavior under SU(3). It behaves like the I = 0, Y = 0 component of an octet, like the Λ in the baryon multiplet (Y is the hypercharge quantum number and is given by the sum of the strangeness and baryon number of a particle). From this definite behavior we can derive mass formulae, relationships between coupling strengths, and so on, all of which are confirmed by experiments. However, we have as yet no knowledge of the nature of this symmetry-breaking effect. I have conjectured that it represents an additional "Fifth" interaction whose strength lies between the strong and the electromagnetic forces. Many of my colleagues think, however, that it is an intrinsic part of the strong force, whose symmetry is thus "spontaneously" broken.

Electric charge is proportional to one of the eight conserved charges of unitary spin; N. Cabibbo pointed out in 1963 that the weak vector charges correspond similarly to another two unitary-spin charges. Electromagnetic or weak matrix-elements for baryons or for mesons can thus be related by SU(3) coefficients; the results are in perfect agreement with experiment.

In two papers in 1962 and 1964, M. Gell-Mann suggested a new interpretation of the unitary-spin charges. To avoid the problematics of the definition of approximate symmetries in the strong interactions, he suggested using the electromagnetic and weak charges as a starting point. Unitary spin is then defined as the set of charges arising when we commute the hadron electromagnetic and weak charges. This is like saying, for instance, that the isospin $\bar{p}n$ charge is just the one we observe in beta decay; $\bar{n}p$ is observed in positron emission in nuclei. We then get the remaining $\frac{1}{\sqrt{2}}$ ($\bar{p}p$-$\bar{n}n$) component of I-spin by commuting the above two.

Gell-Mann's identification allowed him to extend the algebra to an SU(3) x SU(3) system of 16 operators, the 8 new charges being identified with the analogues of the weak axial vector ones, a^0. The new group is not a symmetry of the strong interactions since axial charges are not conserved; however, the existence of nonlinear relations in the form of commutators imposes severe restrictions and defines a scale for the axial vector currents. Saying that a set of charges G_i forms an algebra means that we require them to fulfill the commutation relations

$$[G_i , G_j] = i f_{ijk} G_k ,$$

where the f_{ijk} are well-known structure constants defining uniquely the Lie algebra.

The next development was based on the suggestion by S. Fubini and collaborators of a method of calculation for the cases in which the G_i do not generate a symmetry. In such cases, the G_i operating on a one-particle state (e.g., a proton) yields a mixed "rotated" state: instead of yielding a pure neutron, as for the I-spin lowering vector charge, the axial I-spin lowering generator will produce an admixture with many-particle states, such as $(p\pi^-)$, $(n\pi^0)$, etc. Fubini suggested estimating this "leakage" and using it to determine the renormalized strength of the leaking transition. The program was carried out successfully by S. Adler and W. Weisberger in 1965, giving, for instance, a figure of 1.18 G_V for the axial vector strength $|G_A|$, in good agreement with experiment. Many of the results which had first been derived from an attempt to generalize SU(3) by using SU(6) and an even larger SU(12) group turned out to be derivable directly from the algebra of the currents. SU(6) had been suggested as a nonrelativistic assumption of both unitary-spin and ordinary-spin independence for the strong interactions. Of course, relativistic situations generally imply transfer of angular momentum between the spin and the orbital components, and SU(6) could only be applied in static situations where this transfer would not occur. Another SU(6) group known as $SU(6)_W$ was shown to hold in a different set of kinematical situations corresponding to collinear motion. An attempt to formulate a "relativistic SU(6) theory" yielded a negative answer--there is no such theory. However, the most extended algebra of the currents does generate an SU(12) group, and this algebra can be used as an algebra of transition operators, but certainly not as a symmetry. M. Gell-Mann is now extending the formulation and hopes to explain thereby the supermultiplet structure of the spectrum. This further advance in the classification uses a relatively new mathematical tool, the theory of unitary infinite-dimensional representations of noncompact groups. In 1965 at Cal Tech, we showed how these structures could be used to represent sequences of excited levels, like the rotational levels in nuclei. The Regge-recurrences in hadron physics appear in similar sequences which have indeed been observed.

More recently, we have been attempting to use the algebraic machinery for a better understanding of the strong interactions themselves. S. Fubini and his collaborators in Turin have introduced the method of superconvergence, in which the low-energy

couplings of the strong interactions are shown to obey very restrictive relations connected with the convergence properties of the algebraic generators' matrix elements. There is some hope that this will connect with another attempt, initiated by N. Cabibbo, L. Horwitz and myself last summer at CERN, which amounts to an algebraic statement of a law-of-force for the high-energy part of the strong interactions. We have been able to reproduce a long list of observed regularities of high-energy cross sections by assuming that they are mediated by two nonets of Regge trajectories with $1^-, 3^-, \ldots$ and $2^+, 4^+, \ldots$ meson poles, respectively. The factorized effective couplings to these trajectories (remember that factorization is allowed here) again form a set of "charges" corresponding to another U(3) x U(3) algebra. To a certain extent this is again a jj^+ picture, except for the Regge dynamics.

The algebraic method has yielded a greater understanding of the physics of hadrons. This is certainly no more than a limited sector of particle physics, and problems such as the spectrum of leptons or the CP noninvariance in neutral K decay seem to lie outside of this exploration. However, we can at least hope to have in some not-too-distant future a good partial theory describing the strong, weak, and electromagnetic interactions of baryons and mesons. ✪

EDITOR'S NOTE:

For further reading on progress in particle physics, the following articles are suggested:

(1) Ne'eman, Y., "Particle Symmetries," International Science and Technology, March 1963.

(2) Ne'eman, Y., "What's Happening in Particle Physics," International Science and Technology, March 1967.

(3) Chew, G. F., M. Gell-Mann and A. H. Rosenfeld, "Strongly Interacting Particles," Scientific American, February 1964.

Dr. Yuval Ne'eman received his B.S. and Diploma in Mechanical Engineering from the Israel Institute of Technology, Haifa, in 1946. His subsequent work in hydrodynamics design was broken off for service as an Israeli infantry commander, in which assignment (in 1955) he achieved the rank of Colonel. In 1958, while in London as Military Attaché from Israel, he decided to do research in physics. Consequently, he left his diplomatic post in 1960, and he received his D.I.C. (1961) from the Imperial College of Science and Technology, and his Ph.D. from the University of London. He later headed the Israel Atomic Energy Laboratories, and has been a Visiting Professor at the California Institute of Technology, Pasadena, and at the Southwest Center for Advanced Studies, Dallas, where he holds a permanent external appointment. He has also been Professor of Physics at Tel-Aviv University since 1965, heading up the Physics Department. In 1966 he received a D.Sc. hon.causa from the Israel Institute of Technology and, in the same year, was awarded the Weizmann Prize for Natural Sciences. He is a member of the Israeli Academy of Sciences and the Israeli Atomic Energy Commission.

Dr. Ne'eman is the co-discoverer of Unitary Spin (or Unitary Symmetry, also known as "The Eightfold Way") with Dr. M. Gell-Mann of the California Institute of Technology. This theory was suggested independently and simultaneously in London and Pasadena by the two scientists, in 1961; it was spectacularly verified early in 1964 with the discovery of the Omega Minus particle in a Brookhaven experiment. Gell-Mann and Ne'eman have reviewed the theory in a book, The Eightfold Way, published by Benjamin.

Since 1961, Dr. Ne'eman has continued to work in particle physics. In 1962, with H. Goldberg, he suggested a triplet-field model with fractional baryon number for the system of strongly interacting particles, an idea whose further development (by M. Gell-Mann and G. Zweig) is now known as the "quark" model. With Y. Dothen and M. Gell-Mann, he has initiated an interest in noncompact groups. More recently, with N. Cabibbo and L. Horwitz, he has suggested an algebraic interpretation of high-energy scattering.

Dr. Ne'eman's work on an algebraic approach to elementary-particle dynamics is sponsored by AFOSR.

cloud rows over Florida

METEOROLOGY LABORATORY, AFCRL

Looking down at cloud patterns over the Florida peninsula, the airline passenger often sees a curiously geometrical arrangement of small, fluffy cumulus clouds. He sees evenly spaced rows of cumulus clouds, like cotton planted in a giant field stretching to the horizon, and may note that the cumulus elements along each row are distinctly separated from one another. Such row-type, pattern-form clouds are not peculiar to Florida; but because they occur there so frequently and with such a well-defined geometry, the Florida peninsula offers an outstanding location to study them.

Mr. Vernon G. Plank, an atmospheric physicist with the Cloud Physics Branch, Meteorology Laboratory, AFCRL, completed Army Air Corps meteorology training programs at the University of Michigan (1943) and Chanute Field, Ill. (1944), and received his A.B. in Meteorology from the University of California at Los Angeles (1949). He took his M.S. in Meteorology at the Massachusetts Institute of Technology in 1954, and has fulfilled the course requirements for the Ph.D. in Meteorology at M.I.T. Since joining AFCRL in 1951, Mr. Plank has conducted various investigations in the general fields of radar meteorology and cloud physics. He has been especially concerned with the radar characteristics of clouds, with spurious echoes on radar, with the refractive-index structure of cloudy regions, and with cloud effects on the radio guidance of space vehicles.

For the past 10 years, a group of AFCRL meteorologists have carried out summer expeditions to Florida to observe all aspects of weather formation over the peninsula and the adjacent Atlantic, Caribbean and Gulf of Mexico region. Instrumented weather aircraft have a large role in these expeditions. Because of the Air Force's heightened interest in tropical meteorology, these studies have assumed increased importance. Vernon G. Plank of AFCRL has focused his attention on "cloud rows" and the conditions favoring their formation. He has recently published his findings.

Cloud rows begin to form along the coastline at about 8:30 a.m. after the earth has absorbed heat from the sun. However, they are observed most frequently and cover the greatest area during the early morning hours and in the middle-to-late afternoon, when they sometimes extend across the entire peninsula. They are relatively infrequent during midday, often disappearing, only to reappear again in the afternoon after the time of maximum surface temperatures. By 5:00 p.m. the geometric row pattern has broken up.

Each cumulus element may be only a few hundred feet from base to top. Sometimes the base is at an altitude of only about 500 feet, and rarely is the base higher than about 3,000 feet. The rows themselves are usually closely spaced at the time of initiation--about 1,000 to 1,500 foot separation. The distance between rows may increase to 10 to 15 thousand feet in the late afternoon. Frequently, the geometrically spaced rows will break up, losing their precise patterning to assume a random arrangement. When this happens, the breakup occurs more or less simultaneously over large regions of the peninsula, encompassing both coastal and interior regions. But, just as often as not, given the same apparent meteorological con-

ditions, the cumulus elements do not arrange themselves in a pattern at all.

From all this it would seem a relatively simple matter to isolate those factors which give rise to cloud rows and those that do not. It would further seem that winds would be the controlling factor. Plank's study was largely concentrated on the wind profiles and wind shears that existed during pattern-form and nonpattern-form conditions.

What were the findings? First of all, cloud rows are most likely to form when winds are in excess of 10 knots, and the rows tend to be parallel to the direction of the wind. More precisely, they tend to be oriented about 3 degrees to the left of the surface wind, and about 15 degrees to the left of the wind at the cloud-base level. But this is only a general characteristic--not a consistently uniform one. Cloud rows were sometimes observed with surface winds of less than 5 knots and at all angles to wind direction.

Plank also investigated the possible effects of the wind-profile curvature--that is, the changes in wind shear with altitude. It had been proposed by others that, if wind shear first increases with altitude and then decreases at a still higher altitude such that the resultant profile curvature is of a certain radius, then there is a strong likelihood of cloud-row formation. Plank found no consistent relationship in these profile curvatures with cloud rows.

Thus, what started out to be a rather straightforward analysis proved to have unsuspected complexity, all of which caused Plank to conclude that his rather gross wind measurements may have lacked the accuracy and resolution required to discern the essential differences in wind structure that sometimes create row clouds and sometimes do not. He suggests that future studies should also take more fully into account the thermal structure of the lower atmosphere.

It is hoped that future AFCRL investigations will lead to a definitive model of the formation of these interesting cloud patterns. ✪

Figure 1. Typical pattern-form cloud geometry over Florida.

Organosulfur Intermediates

DR. ANTHONY J. MATUSZKO
Directorate of Chemical Sciences, AFOSR

One of four research chemists from the United States invited to present a lecture at the Second International Sulfur Symposium was Dr. Henry Shine of Texas Technological College. The Symposium, which covered recent developments on the chemistry of reactive organosulfur species, was held at the University of Groningen, Holland, 9-12 May 1966. Dr. Shine talked about his research on the mechanisms of formation and identity of thioaromatic cation radicals, work which has been supported for the past few years by the Directorate of Chemical Sciences, AFOSR. He discussed also the correlation of the data obtained by his research group--by means of electron-spin-resonance spectroscopy, absorption spectroscopy, nuclear-magnetic resonance, and product studies--to form a general understanding of the systems being studied. While the descriptive chemistry has been known for some time, the characterization of Shine and co-workers of the species involved has been much more recent and, indeed, quite new to many chemists. This presentation will be incorporated into a book based on material from the Symposium to be published by John Wiley and Sons.

What is this strange breed of compounds labeled "thioaromatic cation radicals," and how does a research chemist like Dr. Shine become involved in this type of work? In the late 1950s, interest in the benzidine rearrangement (a reaction in which hydrazobenzene, $C_6H_5\text{-}\overset{H}{\underset{|}{N}}\text{-}\overset{H}{\underset{|}{N}}\text{-}C_6H_5$, rearranges in acid solution to benzidine) led Shine to investigate the rearrangement of the thioaromatic analog diphenyldisulfide, $C_6H_5\text{-S-S-}C_6H_5$. It had already been shown some 50 years earlier that diphenyldisulfide, on treatment with 100% sulfuric acid, is converted to water-soluble products and a small amount of thianthrene (I).

How was the thianthrene formed? It was known that thianthrene, as well as thianthrene 5-oxide (II), formed the same radical in sulfuric acid. The problem was to find the structure of the radical and show how it was formed. Shine was convinced that an interpretation of the chemistry of the thianthrene system would be applicable to most organic sulfides and their oxides. Absorption spectroscopy, product analysis, and electron-spin-resonance spectroscopic evidence obtained in his laboratory led Shine to propose the structure for the thianthrene cation radical (III) which is now universally accepted.

The reaction of thianthrene itself was found to be a simple one, a one-electron oxidation:

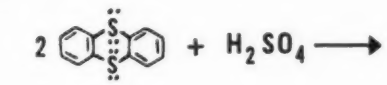

I

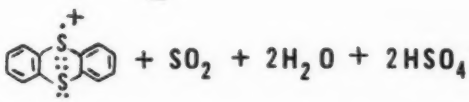

III

Much more startling was the finding that, since the same radical was formed from thianthrene 5-oxide, that compound had to become deoxygenated in concentrated sulfuric acid. The proposed mechanism for the deoxygenation reaction together with observed dication (V) formation is given below: (See also Fig. 1)

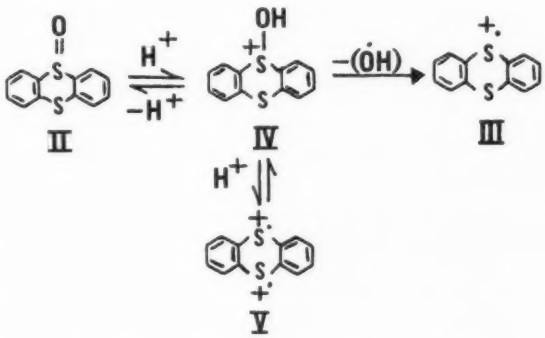

Dr. Shine and his co-workers have now shown that the deoxygenation reaction is a general one for certain classes of aromatic sulfoxides. It occurs in the phenothiazine

series (where the S without the oxygen in thianthrene is replaced by N-H). This type of chemistry is of considerable interest because of its connection with the in vivo action and breakdown of animal and human drugs based on phenothiazine. Shine's mechanism for the deoxygenation studied in 45% sulfuric acide is similar to that shown for II above (except for the dication formation observed in concentrated sulfuric acid).

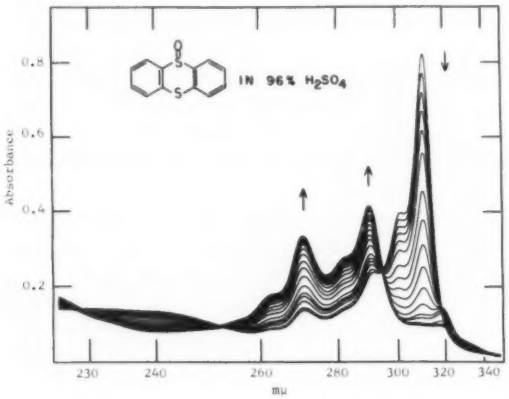

Figure 1. UV spectra for changes in thianthrene 5-oxide(II). The downward arrow shows the decrease of a peak at 310 mμ. This peak corresponds with the thianthrene dication (V). The upward arrows show the growth of peaks at 271 and 290 mμ. These peaks are due to the thianthrene cation radical(III). The change in spectrum took place over a period of 3 days.

The Texas Tech research team is the only group which has tackled the cation-radical chemistry in such an analytical way. So far, cation radicals and dications have been characterized. What is needed now is a study of the reactions of these unusual reactive sulfur intermediates. Will cation radicals initiate polymerization, for example, and form the type of living polymers now well known in anion radical systems? What sort of oxidizing agents are these species? Where will they undergo radical and nucleophilic attack?--on sulfur or on an attached ring? The research is currently directed toward coming up with answers to these questions. The results obtained could benefit the Air Force in providing a better understanding of the effect of aerospace-environment high-energy radiation on sulfur-containing substances, such as body proteins. Should the cation radicals be successful initiators of polymerization, they may provide the Air Force with a new and interesting route to the synthesis of block and graft polymers.

ALBEDO CONTRIBUTIONS TO THE IONOSPHERE

UPPER ATMOSPHERE PHYSICS LABORATORY, AFCRL

Reflected sunlight from the earth may play a much larger role in the ionization of the D and E layers of the ionosphere than is usually supposed. When sunlight is reflected from clouds or snowcover, ionization rates may double the rates found over oceans or darker land areas.

T. J. Keneshea, G. J. Gassmann and W. Pfister of AFCRL have recently reported on the contributions of reflected solar radiation to ionization in a paper, "The Effect of Varying Albedo Radiation on the Ionospheric D-Layer." The paper discusses a computer model developed for the IBM 7094 which takes into account all known photochemical processes in the D and E regions.

Let's look at these processes briefly. The ionospheric D layer is created by solar photons, with an important part of the resultant chemistry being photodetachment processes. The solar radiation initiating this process falls primarily in the visible region. For example, if we take one atmospheric molecule, the oxygen ion O_2^-, the solar photon knocks off an electron leaving O_2 and a free electron. We tend to think of the photons as coming directly from the sun--and, in fact, most do--but, through Rayleigh scattering, they can arrive at the oxygen molecule from all directions. And, as we noted above, they can come from the earth in the form of reflected sunlight.

The negative-ion molecule, O_2^-, is found in sizable concentrations in the D layer; its

Mr. Thomas J. Keneshea (left), and Dr. Wolfgang Pfister (right) are both with the Atmosphere Structure Branch, Upper Atmosphere Physics Laboratory, AFCRL. Mr. Keneshea, a physicist, has a B.S. in Physics from the University of Rhode Island (1949), and an M.S. in Physics from Brown University (1952). He has been with AFCRL since 1951, and is presently engaged in research on the physics of the ionosphere.

Dr. Pfister, a senior scientist, has the degree of Dipl. Ing. (1929), and the degree of Dr. Ing. (1934), both from the Technical University of Munich. He has conducted research in the field of tropospheric and ionospheric radio propagation, and is currently considering the problems of electron and ion density in the ionosphere. Dr. Pfister has been with AFCRL since 1948.

photodetachment coefficient of electrons has been examined by others. Under full direct sunlight, without accounting for earth-reflected sunlight or Rayleigh scattering, the photodetachment coefficient is 0.44 per ion per second. Previous studies have also shown that at 65-km altitude above thick cloud cover or with fresh snow, this coefficient almost doubles to at least 0.86. The corresponding value over water is 0.53.

Now suppose we wished to examine not just one atmospheric specie, but all of the species found in a particular altitude regime--and not just one type of reaction, such as photodetachment, but all associative-dissociative dynamics that are in a continuous process of ionizing and deionizing the atmosphere. For this, the AFCRL scientists have turned to a mathematical model. With such a model, assuming a good computer program

and valid inputs, we can vary parameters and obtain a clear picture of the dynamic chemical processes of the D layer.

The AFCRL computer model deals with 15 atmospheric species simultaneously, and uses the rate coefficients of about 150 different processes, taking into account diurnal variations. To verify results, they are compared with known variations of the D and E regions. With this basic model, the amount of reflected sunlight can be varied and effects on the ionosphere studied.

The AFCRL scientists were particularly interested in radio-wave absorption; this factor also is a part of the computer model. They found that, under highly reflective conditions, when a 3-MHz signal is transmitted through the ionosphere (as in satellite transmissions to the ground), absorption increases from the nonreflective case to the reflective case from 15.5 to 19.4 db. If a ground-based radiometer at 3-MHz is used to reflect a signal from the ionosphere, the expected decrease of echo field strength is 7.8 db when the light flux is doubled due to albedo.

From this, it would seem that if one wishes to measure the effects of the albedo on the ionosphere at a given time and place, then all that is necessary is to set up a radiometer and measure the echo field strength. For many reasons, it is not as simple as that. The continuous undulating and varying ionospheric densities will give wide variations in the received signal. But a fast-moving vehicle, such as an airplane or a satellite, does offer the possibility of making variable albedo measurements in quick succession while signal characteristics remain constant. AFCRL, with a KC-135 aircraft instrumented for ionospheric research, and a large satellite instrumentation program, is well equipped to make such measurements in the future.

magnetic field geometrics in a tank

SPACE PHYSICS LABORATORY, AFCRL

Fashioning the desired intensity and geometry of a magnetic field is a job of some mathematical magnitude--even for a computer. But if less than extreme precision is acceptable (and for many experiments it is), then the geometries of these fields can be designed rather simply by simulation in an electrolytic tank. This is because the current density in an electrolytic fluid has a direct relationship to magnetic-flux density in space.

Electrolytic-tank simulation of magnetic fields was recently discussed in a paper by Lewis Combes, Charles C. Gallagher, and Morton A. Levine of AFCRL. They have designed an electrolytic tank to simulate the magnetic field that would be generated by a given segment (Figure 1) of toroidal field coils.

The electrolytic-tank analog of this field-coil segment consists of a shallow, wedge-shaped Plexiglas rectangular box. Inside, the area is divided into sections by means of narrow rectangular blocks representing the field coils. Partitions separate the copper-foil electrodes. Connections are made to the electrodes at five locations. The resultant tank design (Figure 2) looks somewhat like a cutaway model showing the room arrangement of a house.

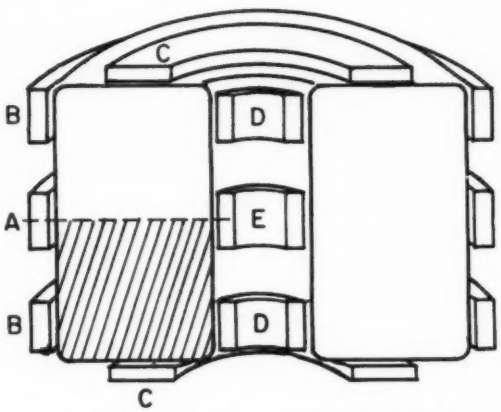

Figure 1. Cross section of toroidal chamber with field coils. Shaded area shows the portion of the chamber simulated in the analog tank.

If current is flowing in the electrolyte

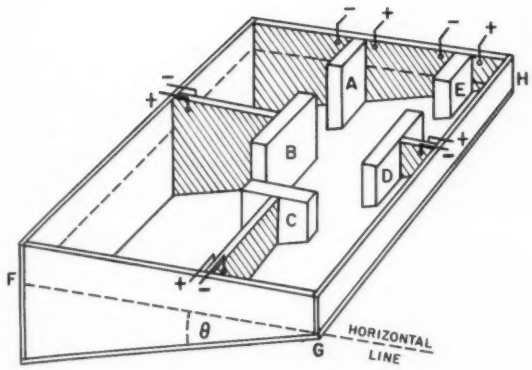

Figure 2. Analog tank with simulated field coils.

(copper sulfate in the AFCRL experiment), the flow lines around the "coils" in the tank simulate the magnetic field that is formed around the coils in the toroid, and point for point the current density in the electrolyte is directly proportional to the magnetic-flux density in the toroid.

In using the analog tank, alternating current is sent through the electrolyte from five separate sources. A means of varying the currents at each of the five sources is provided by a rheostat.

The result is the simulation of magnetic fields in a vacuum. But, if the toroidal field

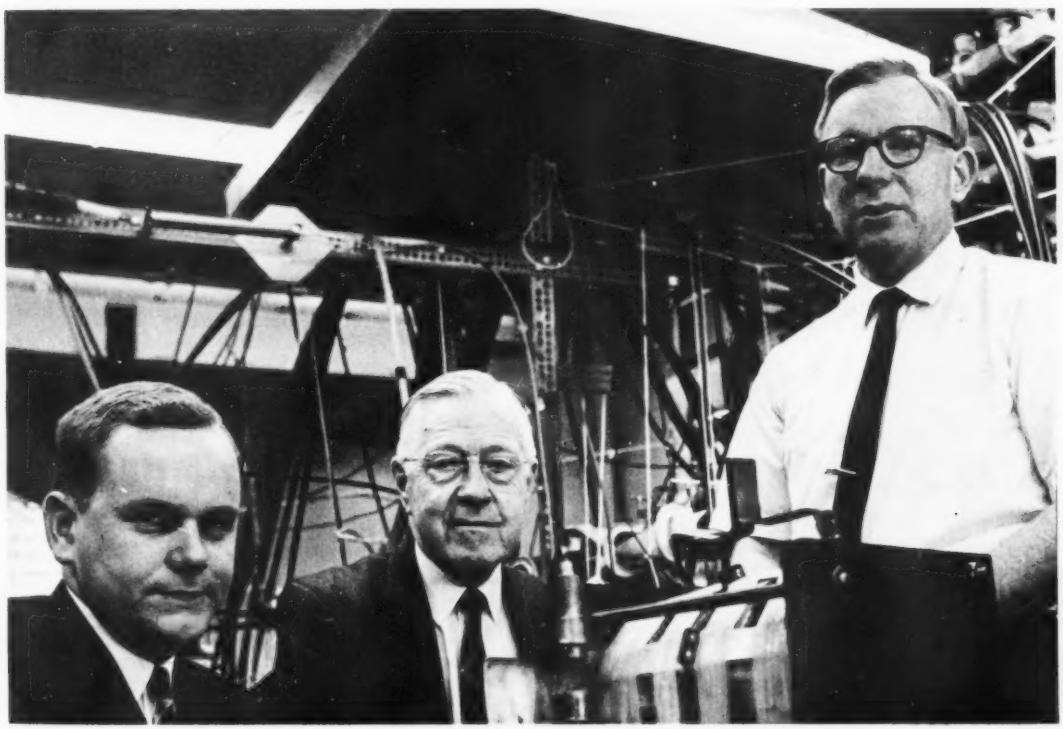

From left to right, Mr. Charles C. Gallagher, Dr. Lewis S. Combes, and Mr. Morton A. Levine, all of the Plasma Astrophysics Branch, Space Physics Laboratory, AFCRL. Mr. Gallagher received his B.S. (1958) and M.S. (1960), both in Physics, from Boston College. He is continuing his graduate study at Northeastern University. Dr. Combes received his B.S. in Physics from Wesleyan University in 1921, and his M.S. at Boston University in 1928. He later returned to that University for graduate work in spectroscopy, receiving his Ph.D. there in 1939. He joined AFCRL in 1959. Dr. Combes and Mr. Gallagher are investigating plasmas in strong magnetic fields. Mr. Levine, Chief of the Plasma Astrophysics Branch, received his B.S. in Physics from the University of Massachusetts in 1947. In 1949 he became a graduate student at Tufts University, where he was awarded his M.S. in Physics. He is a candidate for the Ph.D. in Electrical Engineering at Northeastern University. He joined AFCRL in 1954. Mr. Levine was a member of the team that first experimentally verified magnetohydrodynamic waves in gas. He is currently investigating the emission and absorption of visible and infrared radiation by dense plasmas as a diagnostic technique.

coils surround a plasma, there would, of course, be a different magnetic-field geometry because a trapped, highly ionized plasma tends to exclude the magnetic field. To simulate such a plasma, the AFCRL group simply used modeling clay, which was placed in the appropriate section of the tank. The clay was shaped to conform to the particular magnetic field being generated. This was done largely on a cut-and-try basis.

What one must achieve in modeling this "plasma" is an equal and uniform current density everywhere on the "plasma" surface--which is the analog of the pressure balance of the magnetic field around a real plasma. To achieve this pressure balance, the electric current flowing around the "coils" can be varied, the size and position of the "coils" can be changed, or the clay "plasma" can be trimmed or reshaped. It was found, however, that the various aspects of the problem converge rather quickly on a solution.

Measurements are made of the electric-field strength in the electrolyte at different parts of the tank. For these measurements a probe, consisting of 2 small wire electrodes about 5 mm apart and dipping a few millimeters below the surface of the electrolyte, is used. The potential difference between the wires divided by the distance between them gives the electric-field strength. The probe must be mounted so that it moves about freely, rotates 360 degrees, and always dips the same distance below the surface. A simple planograph can be used for this purpose.

Electrolytic-tank modeling of magnetic fields, per se, is not an original concept of the three AFCRL scientists. But they have extended, modified, and simplified the concept to the point where it has become a highly useful part of magnetic and plasma research instrumentation at AFCRL. ✪

conference on intelligent systems

ROWENA SWANSON, Directorate of Information Sciences, AFOSR

"Artificial intelligence" has become a popular term for referring to research across many disciplines that relates to incorporating into machines the ability to perform operations that are generally associated with human intelligence.

An invitational "Conference on Intelligence and Intelligent Systems" was sponsored by the Air Force Office of Scientific Research at the University of Georgia, January 16-18, 1967. The Conference provided a forum to review many of the approaches that are being developed toward designing intelligent machines.

In opening the Conference, Brigadier General E. A. Pinson, Commander of the Office of Aerospace Research, noted that "intelligent systems--systems that can learn, systems that can adapt, systems that can function reliably in hostile environments--are systems that can enhance the Air Force operational capability."

The Conference was designed for the interchange of ideas between long-time and recent contributors to the field. No formal papers were presented, but the sessions consisted of panel and question-and-answer comment discussions. There were four scheduled panels. Participants and topics were:

Session 1. "Foundational Considerations for the Conference," Rowena Swanson (AFOSR), Chairman; Lee Brissey (Oregon U), Richard Gregory (Cambridge U), Seymour Papert (MIT), Charles Rosen (Stanford Research Institute (SRI)), and Marco Schutzenberger (Institut Blaise Pascal), panelists.

Session 2. "Representations and Modeling in Problem Solving," Saul Amarel (RCA), Chairman; Thomas Evans (AFCRL), Edward Feigenbaum (Stanford U), Manfred Kochen (Michigan U), and Seymour Papert (MIT), panelists.

Session 3. "Approaches to Machine Intelligence," Bertram Raphael (SRI), Chairman; Robert Larson (SRI), Nils Nilson (SRI), Robert Minnick (Montana State U), and Robert

Simmons (System Development Corp), panelists.

Session 4. "On the Structure of Human and Machine Intelligence," John Sanders (Brandeis U), Chairman; Daniel Bobrow (Bolt, Beranek and Newman), Hilary Putnam (Harvard U), and Gardner Quarton (Massachusetts General Hospital), panelists.

Topics of sessions on the final day were determined by the Session Chairman based on the discussion and interests of the group. The day's sessions were chaired by Robert Fano (MIT) and Arthur Portor (Toronto U). Allen Newell (Carnegie Institute of Technology), who had been scheduled for Sessions 2 and 3, described his use of heuristics and analytic results of problem-solving protocols. Ross Quillian (Bolt, Beranek and Newman) described a model for simulating inferential characteristics of human memory. Arthur Samuel (Stanford U) outlined recent modifications of his checker-playing program. Stephen Sherwood (Palo Alto-Stanford Hospital Center) related psychiatric data to parameters of intelligence.

Accommodations were arranged by Robert McRorie, Office of General Research, University of Georgia. Publication of the Conference Proceedings is planned as quickly as possible.

a control-systems study of the human eye-positioning mechanism

1ST LT GERALD COOK
Aerospace Mechanics Division, FJSRL

The study of biological systems and efforts to obtain mathematical representations or models of biological systems have received considerable attention recently. Such attention is important to the Air Force because, in designing machines which interact with man, it is necessary to understand the input-output characteristics of man--both over all and perhaps within subsystems. This is important in the medical field because to treat an abnormality one must first understand the normal behavior. Then too, models are important in the education field because of their value as teaching aids.

A study (1-3) has been made of the human eye-positioning mechanism with the objective of obtaining a realistic representation of the system, i.e., one in which each model parameter has a physical counterpart. This is in direct contrast to treating the system as a black box and obtaining a model which merely matches input-output characteristics.

For the investigation, a basic configuration of a controller driving a dynamic plant was assumed. Such a division seems quite natural with the human brain being taken as the controller, the nerve signals being the control variables, and the eyeball, extraocular muscles, and orbit composing the plant.

The over-all behavior of this system was investigated through eye-tracking experiments in which the target moved in a horizontal plane and the subject moved his eyes in an effort to follow the target. The plant itself was investigated through a literature search which was directed toward identifying and mathematically describing the various components of the plant through physiological and anatomical considerations. The shape of the control signals was estimated from electromyograms, i.e., recordings of nerve activity within the muscles. The plant was then simulated on a computer and driven with control signals of the form estimated from the electromyograms. By comparing the movement behavior obtained from the simulation with the actual movement behavior as measured experimentally, the validity of the model was confirmed. Comparisons were made not only of displacement but also of velocity, thus providing a more severe test than displacement comparisons alone.

It was found that the plant is quite slow and highly overdamped, with most of the damping residing in the extraocular muscles, and that this damping is proportional to the control signals of the respective muscles.

The damping effects within the shortening and lengthening muscles were found to be quite different. For this reason a complete description of control behavior requires that one know not only the difference in the control

and 5 in. in diameter, while detector C is 8 in. long and 8 in. in diameter.

Simple angular distribution measurements are made by recording γ-ray spectra in detector C at various angles θ_V. A triple-correlation measurement results if only those parts of the spectra are recorded that are coincident with γ rays of a selected energy in a fixed detector. By using 2 fixed detectors and setting up coincidence gates over 2 different γ-ray energies in each, 4 separate triple-correlation experiments can be per-

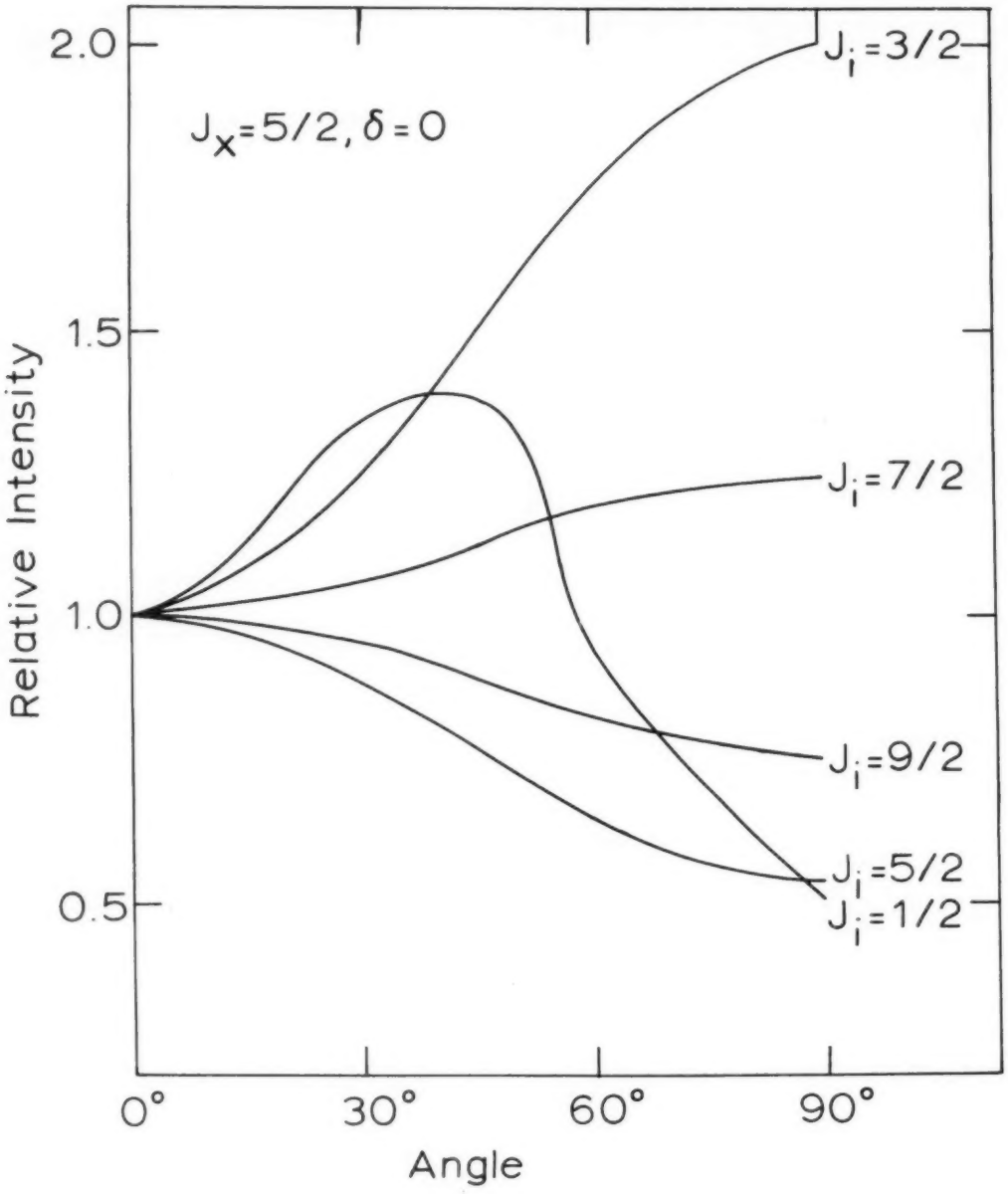

Figure 2. Theoretical angular distribution for $J_x = 5/2$ and $\delta = 0$.

formed simultaneously. In the present work, detector A was always at 90° to the beam direction, whereas detector B was at $\theta_f = 90^\circ$ for some measurements, and at $\theta_f = 135^\circ$ for others.

To illustrate how powerful this method is, two figures have been included, showing some theoretical angular distributions relative to the γ-ray intensities at 0°. An initial state of angular momentum $J_x = 5/2$ is assumed. Figure 2 shows the distributions resulting for different angular momenta J_i of the lower state when only the lowest possible multipole order makes a significant contribution. Figure 3 singles out the case $J_i = 3/2$, and shows the effect of different amounts of admixture

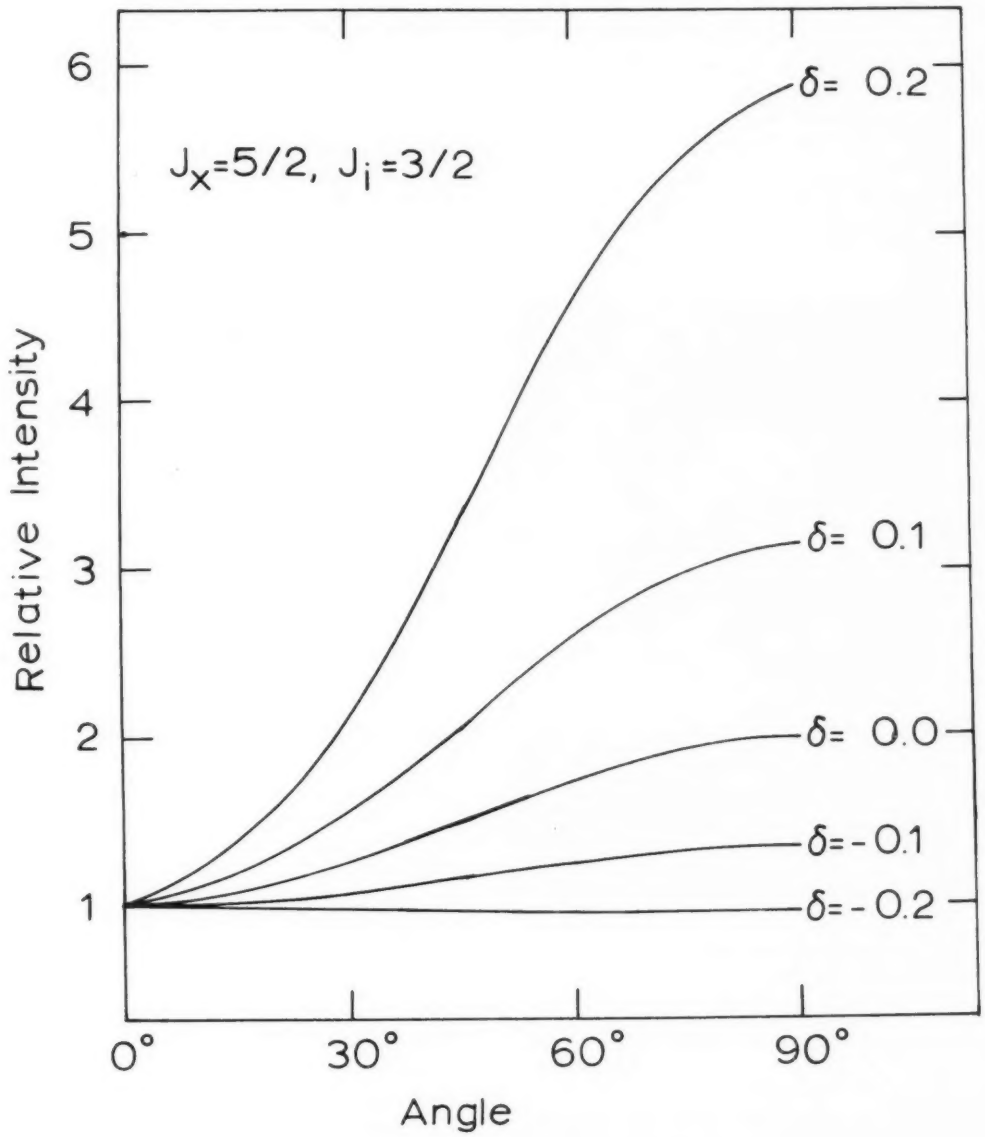

Figure 3. Theoretical angular distribution for $J_x = 5/2$ and $J_i = 3/2$.

of the next higher multipole order, as measured by the "mixing ratio" δ.

It is evident from the curves that the method is not always unambiguous. The values of the relative intensities from the curve for $J_i = 3/2$ and $\delta = -0.12$, for example, would be hard to distinguish from the one for $J_i = 7/2$ and $\delta = 0$. (Note difference in vertical scales for relative intensity.) Evidence from other transitions involving the same levels or from other types of experiments must be used in such cases to make a choice between the possibilities.

REFERENCE

(1) Hyder, Anthony K., "The Study of Nuclear Excited States by Means of the (p,γ) Reaction," OAR Research Review, 5, 6, August 1966.

First Lieutenant Henry Willmes is a research physicist in the Nuclear Structure Group, General Physics Laboratory, ARL. He received his B.S. (1961), M.A. (1962), and Ph.D. (1966) from the University of California at Los Angeles. Upon his being commissioned in the Air Force Reserve in January 1961, he was granted a delay from active duty to pursue graduate studies in experimental nuclear physics. He earned his M.A. under a Link Foundation-Arnold Society Fellowship, and held research assistantships at the UCLA cyclotron laboratory from 1962 to 1965. He was called to active duty in November 1965.

THERMOELECTRIC POWER AND ELECTRICAL CONDUCTIVITY OF NbO_2

JAMES A. ROBERSON, Metallurgy and Ceramics Laboratory, ARL

The occurrence of an electrical potential gradient in a conductor which is placed in a temperature gradient is known as the Seebeck effect. The fundamental equations on which the explanation of the Seebeck effect is based were developed by William Thomson (Lord Kelvin) and relate the Thomson heat to the Seebeck coefficient and the absolute temperature. The Thomson heat was originally considered to be a sort of specific heat of electricity, because it was observed that heat was transported reversibly by an electric current in a conductor which was subjected to a temperature gradient. However, we are now aware that the heat capacity of the conduction electrons is exceedingly small because of the limitations imposed by the Fermi-Dirac distribution function. Therefore the major contribution to the thermal energy transported by the charge carriers arises from the entropy which is transported with them. The flow of entropy has some characteristics which seem to imply that a substance with a finite heat capacity had moved through the conductor. The entropy flow which is associated with the passage of charge (sometimes called "the entropy of transport") from the hot to the cold end of the conductor is a reversible process, and should not be confused with Joule heating or ordinary thermal conduction which are irreversible.

The Seebeck potential is related to the partial molal entropy of the charge carriers and to their heat of transfer. This potential difference is a direct measure of the difference in their chemical potential or partial molal free energy between two points at different temperature. It seems reasonable to believe that the difference in entropy is a result of the different energy states available to the electrons at the two temperatures.

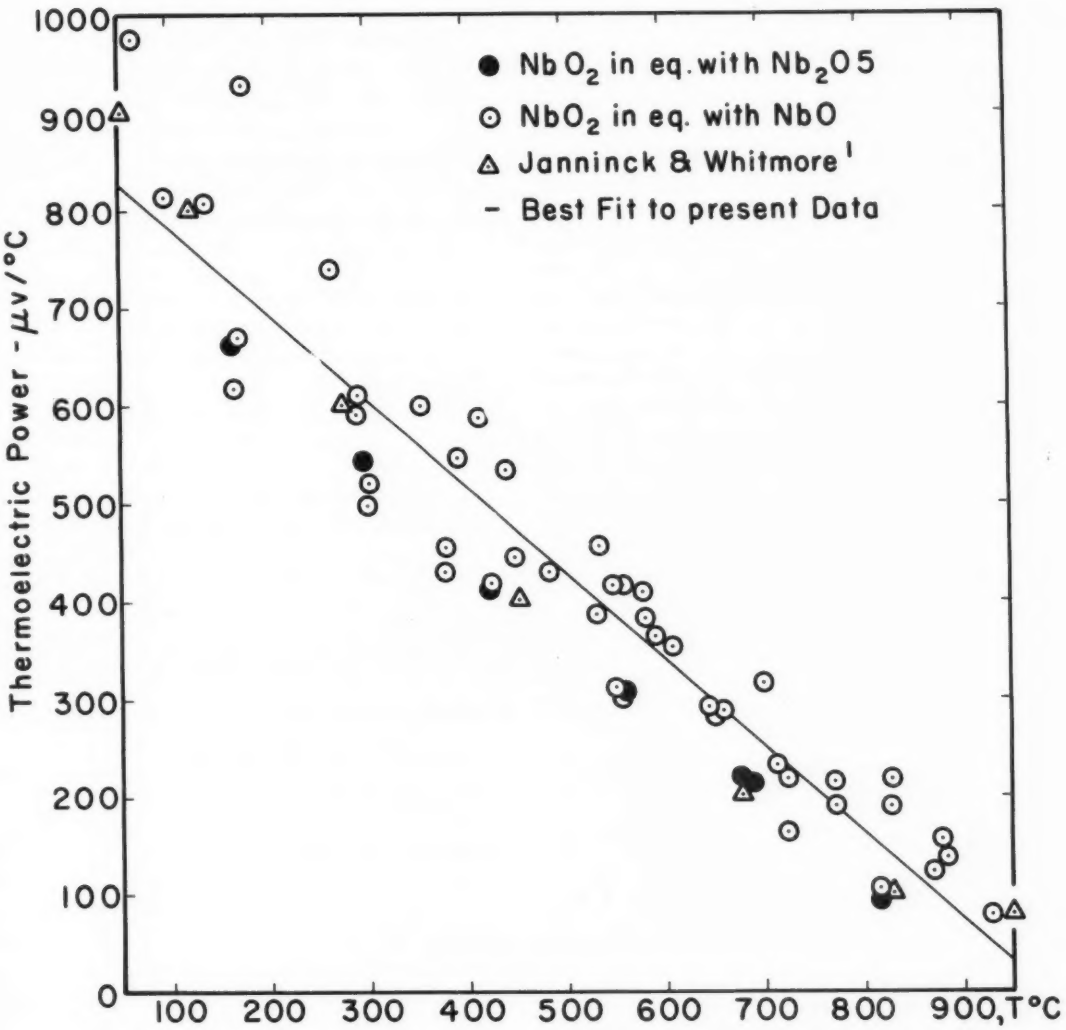

Figure 1. Effect of temperature and oxygen pressure on thermoelectric power of NbO_2.

The greater multiplicity of states at the higher temperature allows a higher configurational entropy contribution.

In a recent paper, Janninck and Whitmore (1) presented data on the electrical conductivity and thermoelectric power of NbO_2 as a function of composition in the temperature range 196 to 1,273°K. The atmosphere which they used was not chosen to provide a stable composition; but the oxygen pressure was low enough to cause a slow reaction rate, and they found the electrical properties of NbO_2 to be insensitive to oxygen pressure. Kusenko and Geld (2) measured the heat content, coefficient of thermal expansion, and electrical conductivity of NbO_2 as functions of temperature. They observed a discontinuous change in Cp at about 1,040°K which may indicate a phase transition of the second kind. This is not surprising in view of the low temperature antiferromagnetism of NbO_2.

The thermoelectric power of NbO_2 is shown in Fig. 1 as a function of temperature at the two oxygen pressures which bound its range of stability.

Expressions relating the density of charge carriers, the absolute temperature, and the thermoelectric power have been derived by Johnson and Lark-Horovitz (3) for semiconductors with various amounts of extrinsic contribution. The equations are greatly simplified if the effects of either electron or positive hole concentration can be ignored. This is possible, of course, if the material is an extrinsic conductor; but it is also possible to make this simplification for intrinsic semiconductors if the mobility of one species greatly exceeds that of the other. This situation is often observed for electrons which have an energy level situated near the boundary of small energy gap (4). It will be shown that the energy gap between the Fermi level and the conduction band in NbO_2 is quite small, so that the use of the simplified relation of Johnson and Lark-Horovitz is probably justified.

$$Q = \pm \frac{k}{e} \left(2 - \ln \frac{nh^3}{2(2\pi m k T)^{3/2}} \right) \qquad (1)$$

where Q = thermoelectric power,
k = Boltzman's constant,
e = electronic charge,
h = Planck's constant,
n = density of charge carriers,
m = mass of carrier, and
T = absolute temperature.

The plus or minus sign is determined by the sign of the majority charge carrier.

This expression can be solved for n (density of electrons) if a value is assigned to m (mass). If m is taken as the rest mass of an electron, equation 1 simplifies to $Q = \pm 0.861\ (10^{-4})\ [38.1 - \ln n + 3/2 \ln T]$. However, this solution, or any other solution, which involves an arbitrary designation of m is open to question. Kittel (4) derives a relation which describes the density of

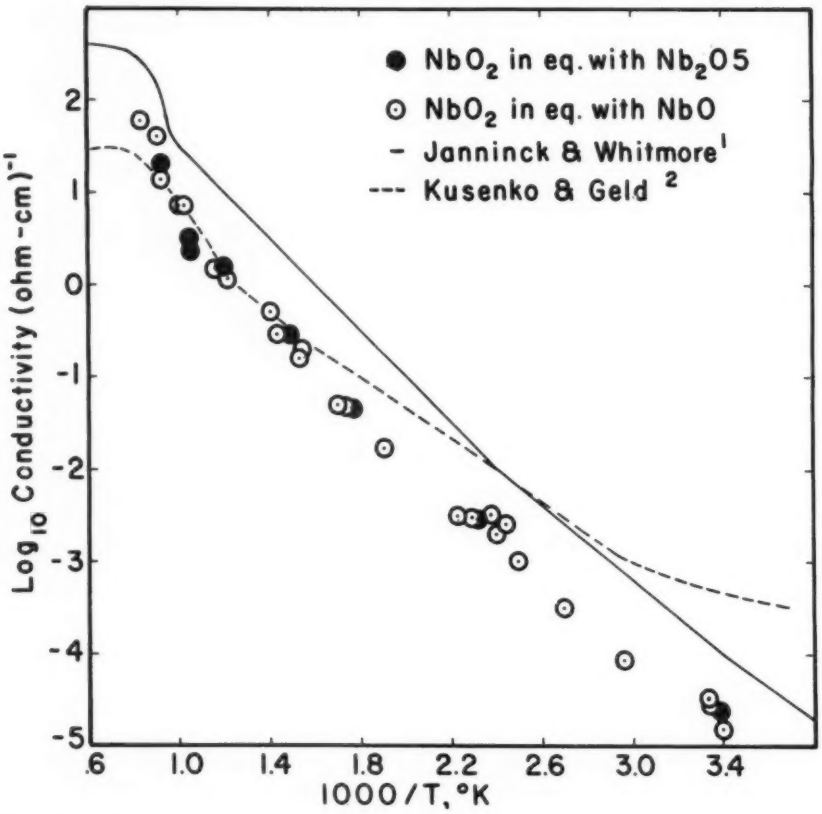

Figure 2. Effect of temperature and oxygen pressure on electrical conductivity of NbO_2.

charge carriers in an intrinsic semiconductor as a function of temperature and the width of the energy gap between free and bound states.

$$N_e = 2(2\pi m k T/h^2)^{3/2} \quad e^{(E_f - E_g)/kT} \qquad (2)$$

where E_f = Fermi energy, E_g = gap between conduction and valence bands. The quantity m can be eliminated from these two equations by solving both of them for ln N and then equating them.

$$\ln N = -Q\frac{e}{k} + 2 - \ln 1/2\left(\frac{h^2}{2\pi m k T}\right)^{3/2} \qquad (1a)$$

$$\ln N = \ln 2(2\pi m k T/h^2)^{3/2} + (E_f - E_g)/kT \qquad (2a)$$

The resulting equation simplifies to:

$$E_f - E_g = T(2k - Qe) \qquad (3)$$

From equation 3 it is possible to determine the energy difference between electrons at the Fermi level and those at the bottom of the conduction band. Three solutions are: E = 0.42, 0.39, and 0.29 electron volts at 400, 600, and 800°C respectively.

The electrical conductivity of NbO_2 is shown in Fig. 2 as a function of temperature and at the two oxygen pressures which bound the range of stability of NbO_2. The results of previous investigators are shown for comparison. It is possible to determine the energy gap between free and bound electrons from the slope of a plot of the logarithm of the conductivity vs. the reciprocal of the absolute temperature. The separation of the valence band and conduction band is 2k times the slope of the plot. The energy gap thus determined was 0.91 electron volts. This result is in fair agreement with those of Kusenko and Geld (2), who found that the width of the forbidden zone was temperature-dependent. Their values were as follows: from 298 to 715°K, ϵ = 0.66 ev; from 715 to 950°K, ϵ = 0.86 ev; from 950 to 1,050°K, ϵ = 1.4 ev.

The Fermi energy is commonly taken to be 1/2 the energy gap computed from conductivity measurements. This value, 0.455 ev, is in excellent agreement with the results computed from the thermoelectric power data, which were 0.42 ev at 400°C and 0.39 ev at 600°C. Such close agreement may be taken as confirmation that the conduction electrons in NbO_2 are thermally activated, which is evidence that NbO_2 is an intrinsic semiconductor. These results were computed for the temperature range in which the log of the conductivity shows a linear dependence on 1/T.

REFERENCES

(1) *Janninck, R. F. and D. H. Whitmore, J. Phys. Chem. Solids, V. 27, 1966, pp. 1183-1187.*

(2) *Kusenko, F. G. and P. V. Geld, Izv. Vysshikh Uchebn Zavedenii, Tsvetn. Met., 3 (4), 1960, pp. 102-106.*

(3) *Johnson, V.A. and K. Lark-Horovitz, Phys. Rev., V. 92, 1953, pp. 226-232.*

(4) *Kittel, C., Introduction to Solid State Physics, New York: Wiley and Sons, 1956, pp. 347-353.*

Mr. James A. Roberson has been a research metallurgist with ARL since 1963, and has been studying the mechanical behavior of metals, particularly regarding fatigue. His investigations have included the variation in the elastic properties of chromium, and a program to determine the effects of stacking fault energy on the work-hardening behavior of face-centered cubic metals. His recent studies of the oxidation behavior of columbium have been directed at identifying and determining the concentration of the mobile ionic defects in the various columbium oxides. Mr. Roberson has a B.S. in Metallurgical Engineering from Purdue University (1956), and is pursuing graduate studies at the Ohio State University. He is a member of the American Society for Metals and the American Institute of Mining, Metallurgical, and Petroleum Engineers.

SPHERICAL-IMPLOSION LAUNCHING TECHNIQUES

JOHN W. GORESH
Fluid Dynamics Facilities
Research Laboratory, ARL

The ballistic range, because of its ability to accelerate a known aerodynamic shape to an accurately known velocity in a variety of atmospheres and under various conditions, has been used successfully for many years to investigate phenomena associated with hypersonic flight. Data obtained from ranges has increased our basic knowledge in the areas of hypersonic aerothermodynamics, vehicle stability, wake structure, and radiative and convective heat transfer, to mention only a few examples. No small effort has been expended to increase the velocity capability of ballistic devices. Propellant-driven guns, which were the first to be used, were limited to velocities of the order of 8,000 to 10,000 feet per second by the low escape speeds of the propellant gases. Later these were superseded by light-gas guns which produced velocities of up to 15,000 to 20,000 feet per second. Finally, multiple-stage light-gas guns were used which could produce velocities up to 30,000 feet per second. The velocities of interest for present space-research problems are well in excess of this limit, extending to 50,000 or 60,000 feet per second and beyond.

The principal problem in extending the velocity limit is that the pressures and temperatures that can be produced and contained in a laboratory apparatus are limited. Working under a contract with the Fluid Dynamics Facilities Research Laboratory, ARL, Prof. I. I. Glass of the Institute for Aerospace Studies, University of Toronto,

Mr. John W. Goresh is currently assigned to the Fluid Dynamics Facilities Research Laboratory at ARL. His present research interests include: (1) turbulent heat transfer due to hot gases flowing through small-diameter cylinders; (2) dissociation of gases at high temperatures and pressures; and (3) reduction of model data at hypersonic speeds. From June 1960 to November 1962, before coming to ARL, Mr. Goresh was at the Dyna Soar Systems Project Office. As Project Engineer under the Dynamics Section, he was responsible for the aeroelastic and dynamic-load design problems encountered in designing the Dyna Soar vehicle. Mr. Goresh has a B.S. in Mathematics from Eastern College, Quincy, Mass. His graduate studies have included mathematics, physics and aeronautical engineering at Boston University, Northeastern University, and Ohio State University, respectively.

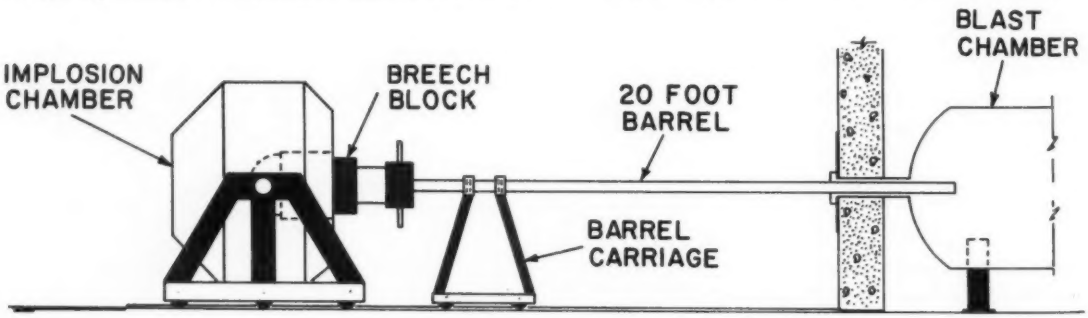

Figure 1. Hypervelocity launcher.

has demonstrated that the current pressure and temperature limit could be overcome by using spherical-implosion waves instead of the planar waves which are the basis for most of the existing launchers. Not only are the peak pressures and temperatures considerably higher (infinite at the origin in the ideal case) than for the one-dimensional case, but they act over smaller interior regions that have limited contact with the containing walls, and hence are easier to contain.

The implosion-driven hypervelocity launcher designed about this concept is shown in Figure 1. It consists essentially of a hemispherical cavity in a massive metal block. A barrel is placed in such a fashion that the entrance to the gun barrel is coincident with the origin of the hemisphere. The interior of the hemispherical surface is coated with a thin layer of explosive, and a diaphragm and projectile are positioned at the entrance to the barrel. The remainder of the hemispherical cavity is filled with a combustible mixture of oxygen and hydrogen.

The principle of operation of the implosion driver can be described briefly in the following manner. The gas mixture is ignited at the origin with sufficient energy to generate a detonation wave in the gas. The detonation wave propagates outward spherically and reflects from the surface of the explosive, igniting it instantaneously and uniformly over its entirety, and generating an explosive-driven imploding shock wave. This shock wave converges toward the center, increasing in strength as it approaches the origin. On reflection it leaves a very high-pressure, high-temperature gas which overloads and bursts the diaphragm; the gas, acting on the base of the projectile, accelerates it along the barrel.

Preliminary experiments with .22-caliber models have demonstrated the feasibility of the imploding-spherical-shock-wave principle. Velocities in excess of 7,000 feet per second were obtained. In several experiments, using small amounts of solid explosives in very thin layers, velocities of 15,000 feet per second have been obtained. Further runs, using a larger (5/16-inch-diameter) projectile have produced velocities up to 18,000 feet per second. The graphs in Figure 2 show: (a) muzzle velocities measured for an 8-inch-diameter hemispherical hypervelocity launcher chamber following the ignition of a 100-psi mixture

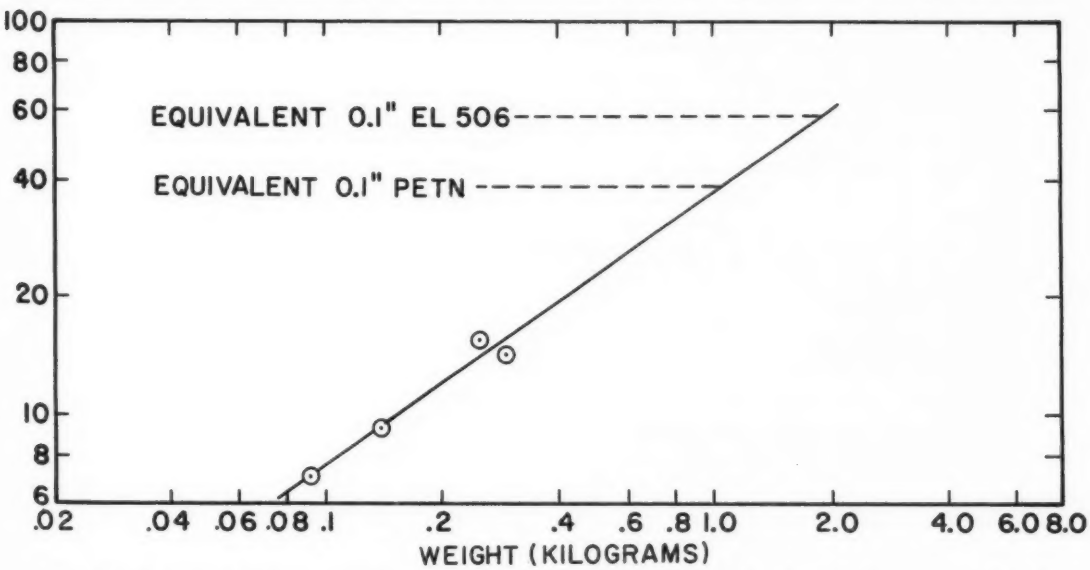

Figure 2a. Measured projectile velocity versus explosive weight for lead-azide liners in an 8-inch-diameter hemisphere at 100 psia initial pressure of stoichiometric oxygen and hydrogen.

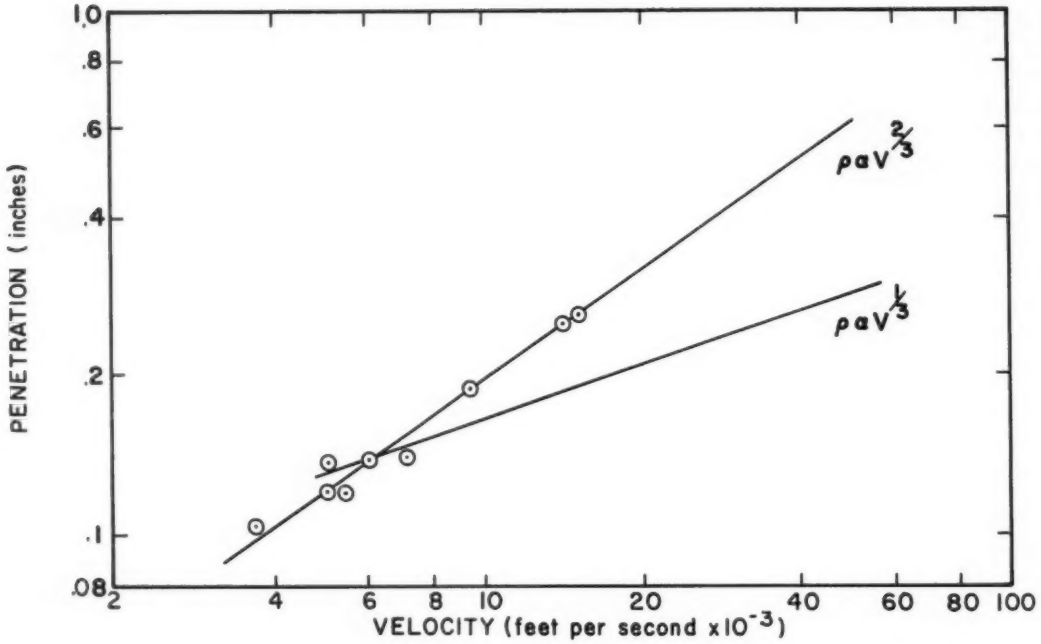

Figure 2b. Measured projectile penetration versus velocity for 0.22-inch-diameter polyethylene cylinders impacting with lead targets.

of stoichiometric oxygen and hydrogen and various weights of lead-azide liner; and (b) a measured projectile penetration versus velocity for 0.22-inch-diameter polyethylene cylinders impacting with lead targets.

Extrapolation to much larger models and to velocities above 50,000 feet per second is now considered to be well within the realm of current technology. The University of Toronto is continuing this work with the construction of a larger-bore hypervelocity gun, capable of launching one-inch-diameter aerodynamic models.

REFERENCES

(1) Glass, I. I. "Shock and Combustion Wave Dynamics In an Implosion Driven Launcher," ARL 65-162, August 1965.

(2) Glass, I. I. "Hypervelocity Launchers, Part II: Compound Launcher-Driver Techniques," ARL 66-0074 (in publication).

Hexagonal Diamond---a New Form of CARBON

DR. WILLIAM L. RUIGH, Directorate of Chemical Sciences, AFOSR

A new crystalline form of carbon, hexagonal diamond, has been synthesized from hexagonal graphite by the application of pressures of 130 kilobars and temperatures of 1,000° C. This accomplishment was recently reported by Drs. F. P. Bundy and J. S. Kasper of the General Electric Research and Development Center. The X-ray crystallographic work was done under contract support of the Directorate of Chemical Sciences, AFOSR.

No normal cubic diamond was formed under the conditions of the experiment; it takes higher temperatures of up to 3,000° C to do so. Hexagonal diamond is formed only when the c-axes of the original hexagonal graphite crystallites are oriented in the press parallel to each other and to the direction of com-

pression. It is not formed from randomly oriented graphite.

The new form of diamond has a crystal structure which is hexagonal and whose unit cell dimensions are a = 2.52 Å and c = 4.12 Å. The density is 3.51g/cm^3, or the same as ordinary diamond. The X-ray diffraction pattern is characterized by two peaks at 2.19 Å and 1.91 Å in addition to the main peaks of ordinary cubic diamond. The high-pressure phase exhibits semiconducting characteristics under pressure, i.e., its resistance decreases as the temperature increases, and vice versa.

If the temperature reached is less than 1,000° C, the material recovered after decompression is the original hexagonal graphite. When the experiment is carried out at a temperature of 1,000° C, the new phase gets "set" so that, on decompression, the material can be recovered in the hard, brittle, hexagonal-diamond form. The diamond material is polycrystalline with an individual particle size of about 0.1μ.

In preparing hexagonal diamond the best starting material was single-crystal Madagascar graphite, although properly oriented pyrolytic graphite (with random orientation along the hexagonal a- and b-axes) can be used. In other studies it was found that oriented specimens of graphite are very strong and completely incompressible in any direction perpendicular to the c-axis.

When this work was almost completed, a Netherlands patent release of duPont revealed that a high-pressure explosive-shock-compression method of preparing diamonds from graphite finely dispersed in a metal matrix gave a product which contains 30% to 50% of hexagonal diamond. The crystallographic characteristics of the duPont material coincide with the General Electric product. On the other hand, diamond material obtained from the explosive-shock compression of graphites by the method of DeCarli and Jamieson contain only microcrystals of cubic diamond.

After the laboratory preparation of hexagonal diamond, it was decided to investigate meteoric diamond material. A specimen of Canyon Diablo "oxide" meteorite was examined, and the diffraction-pattern intensities showed that over 30% of the diamond present was of the new hexagonal type. It is theorized that the diamond was formed from graphite inclusions in the meteorite by impact shock either upon hitting the earth or possibly by earlier collisions in space.

Because of its hardness, this new material is potentially useful as an abrasive and cutting agent for the shaping of hard metals and alloys.

balloon trajectory control and prediction

AEROSPACE INSTRUMENTATION LABORATORY, AFCRL

Not too long ago, balloon-launch crews released their huge polyethylene bags, crossed their fingers, and hoped for the best. Predictions of just where the balloon payload would eventually come down had large conjectural overtones.

But, during the past several years, many refinements have come to the art of balloon-trajectory control and prediction. The art largely consists of taking advantage of varying wind strata in the stratosphere. The skillful flight director, by either gas-valving or ballasting, can effect the slight altitude shifts which are often all that is needed to place the balloon in a more desirable wind stream.

Improved balloon-trajectory control and prediction have come about largely through the efforts of a new kind of specialist--meteorologists who know ballooning dynamics and who have specialized in the study of the wind patterns that affect balloons in flight.

Bernard D. Gildenberg of AFCRL discusses ballooning from a meteorologist's viewpoint in a recently issued report, "Meteorological Aspects of Constant-Level Balloon Operations in the Southwestern United States" (AFCRL-66-706). In describing this specialized role, Gildenberg also provides insights into the ballooning art itself.

AFCRL, at its launch sites at Holloman AFB, New Mexico, and at Chico, California, launches more large research balloons than

any other single agency in the world. Each week, 2 or 3 are sent aloft to altitudes ranging from about 50,000 to 130,000 feet, carrying payloads in support of environmental research programs of AFCRL and other Air Force and Government laboratories.

The balloon meteorologist begins his work on the day before the flight. He already knows the average seasonal and spatial distribution of prevailing winds. This is supplemented by short-range forecasts, his primary tool being the radiosonde. In a sense, he is a practicing micrometeorologist in that he is interested in differences in weather (wind fields) within a space of a few hundred or a few thousand feet. The launch crew usually begins preparation at about 1 or 2 a.m. First the balloon, kept in a sealed shipping crate until this time to avoid moisture absorption which might cause the polyethylene or mylar material to stick together, is uncrated. It is then stretched out (to an 800-foot length in the case of 2 huge balloons launched last year by AFCRL) at a location and in a direction indicated by the meteorologist. Helium inflation takes about 1 hour. Range tracking crews are alerted. The balloon is usually launched between 6 and 8 a.m., when surface winds are at a minimum.

But the launch is made only after the meteorologist has assured the flight director that a range of meteorological conditions is satisfactory--conditions such as surface winds from balloon layout through launch time, cloud coverage at launch and enroute, humidity, temperature inversions and their

Figure 1. The balloon in the foreground is being inflated for launching. The tethered blimp-shaped balloon already aloft in the background gives the meteorologist a constant reading on surface winds. Slightly below and to the left is a radiosonde ascending to give readings on winds aloft.

height, strength and duration, wind speed, shears, tropopause height, wind vectors at float altitude, and many others. From the complex juggling of these variables, the meteorologist predicts the touchdown point of the payload so that the recovery crews can be deployed.

Ideally, of course, a balloon would rise and hover within a radius of a few miles of the launch site. Practically, the goal is to keep the balloon within the range of tracking stations for as long as possible. Also, one would like to avoid sending the pickup crews halfway across the country to recover the payload package.

Gildenberg, in his report, cites many flights where, although certain layers of stratosphere winds have exceeded 100 knots or so, balloons in nearby layers have averaged only a few knots. He cites another case in which 2 balloons, both at the same altitude and only 4 miles apart, were in trajectories carrying them in opposing directions. This is possible in areas where a closed circulation pattern exists. At certain times, usually over deep valleys, such circulations carry the balloon in a large circle completely around the launch site. Several cases of hovering for long periods are noted, the record being 11 days for a balloon launched at AFCRL's Chico, California site.

Control is achieved by ground tracking and altitude adjustment made by radio command. Beyond the present state-of-the-art is an automatic system in which the balloon senses its acceleration when it is caught in a high-velocity wind stream, determines a minimum wind field, and either automatically drops ballast or valves off gas to ascend or descend to an optimum layer. ✪

ATLAS ON ATMOSPHERIC HUMIDITY IN NORTHERN HEMISPHERE PUBLISHED

AEROSPACE INSTRUMENTATION LABORATORY, AFCRL

Recently published by AFCRL is the most comprehensive study on atmospheric humidity that has been issued to date. The study has been published in the form of an atlas, with 120 plates devoted to isopleths of water-vapor mixing ratios and dew points over the entire Northern Hemisphere. The distribution of water vapor over the Northern Hemisphere is of Air Force interest because of the intense absorption by water vapor of infrared energy. The amount of water vapor present in the atmosphere defines the sensitivity limits of infrared detectors.

Data for the atlas were drawn from 1,500 surface observational sites and 400 upper-air radiosonde stations distributed throughout the Northern Hemisphere. More than 60 per cent of these were on the Eurasian mainland. At each station, dew-point data were taken over a five-year period. (Water vapor is measured in terms of dew point, which is the temperature at which air becomes saturated when cooled without the addition of moisture or change of pressure.)

Water vapor, of course, varies with altitude and with season. But even within a season (or from day to day, for that matter) there are wide variations. The atlas takes all this into account. Data for only 4 mid-season months--January, April, July and October--were compiled. For each of these months, isopleths were plotted for 5 pressure levels. These pressure or millibar levels are 850 (470 feet), 700 (9,800 feet), 500 (18,500 feet), and 400 (23,600 feet). But the average monthly values alone at these various layers is a rather coarse index. A set of percentiles representing the frequency distribution of the moisture content, level by level, gives a more meaningful picture. Therefore, at each level for each of the 4 months, separate isopleths are plotted on the percentage of the time one would expect to find a given dew point. Percentiles chosen were 5, 25, 50, 75 and 95.

Twenty of the 120 charts consist of isopleths of mixing ratio at the surface of the earth.

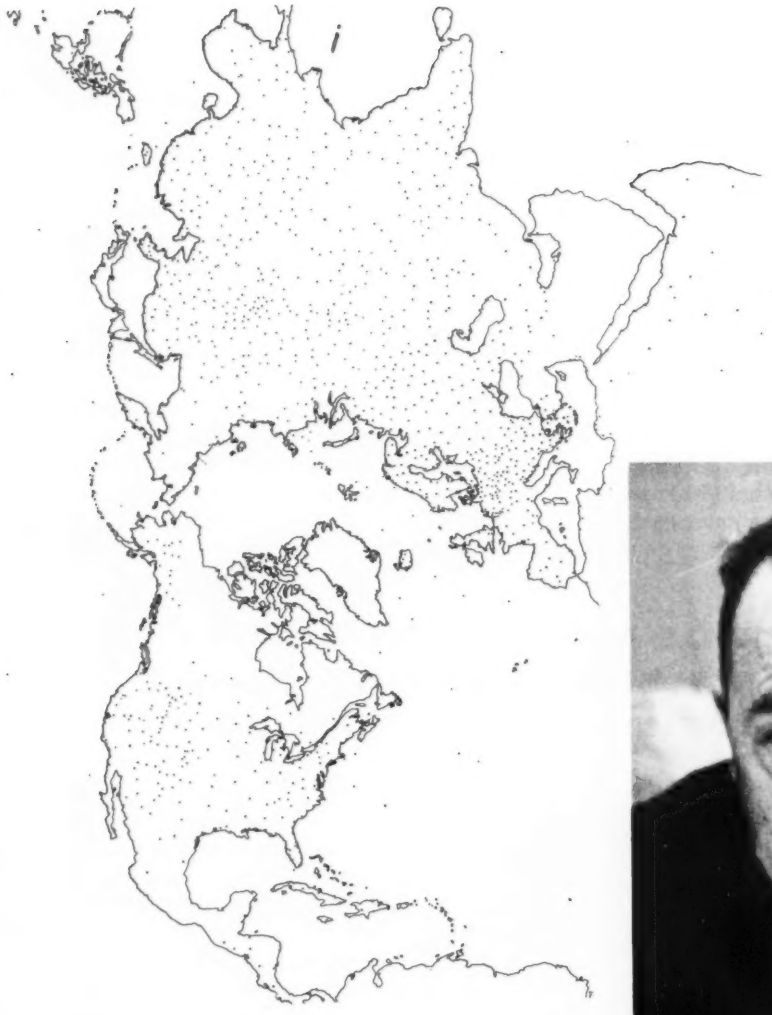

Figure 1. Map of the northern hemisphere showing locations of 1,500 stations where surface observations of atmospheric water vapor were made.

The mixing ratio is the proportion of the mass of water vapor to the mass of dry air.

The atlas was a joint endeavor of the Air Weather Service's Environmental Technical Applications Center, which supplied most of the data, and AFCRL, which analyzed the data and prepared the report. I. I. Gringorten, H. A. Salmela, I. Soloman, and Major I. Sharp are the authors of the atlas.

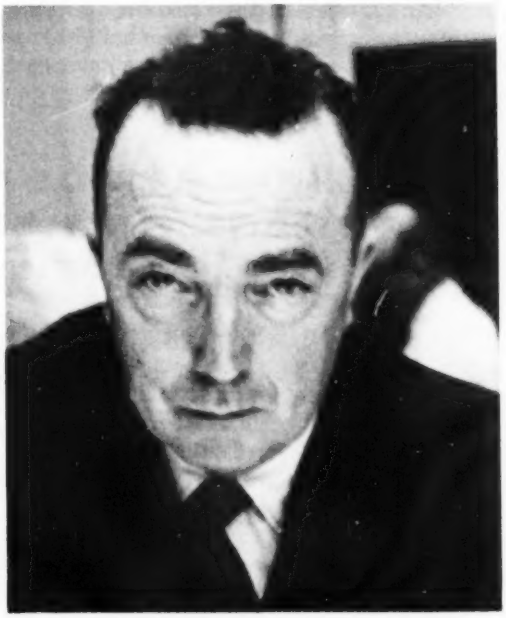

Mr. Henry A. Salmela, a meteorologist with the Design Climatology Branch, Aerospace Instrumentation Laboratory, AFCRL, received his B.S. in Physics and Mathematics from the University of Massachusetts in 1939. He completed an Army Air Corps meteorology program at the Massachusetts Institute of Technology in 1943, and later did graduate work at North Carolina State College and at M.I.T. Mr. Salmela joined the Geophysics Research Directorate, a component of the Air Force Cambridge Research Center (predecessor of AFCRL) in 1949. He is currently studying the variability of winds in time and space, the errors in observing winds, and the errors in their analyses. He is also concerned with water vapor in the stratosphere, and is one of the authors of the atlas on atmospheric humidity described in the accompanying article.

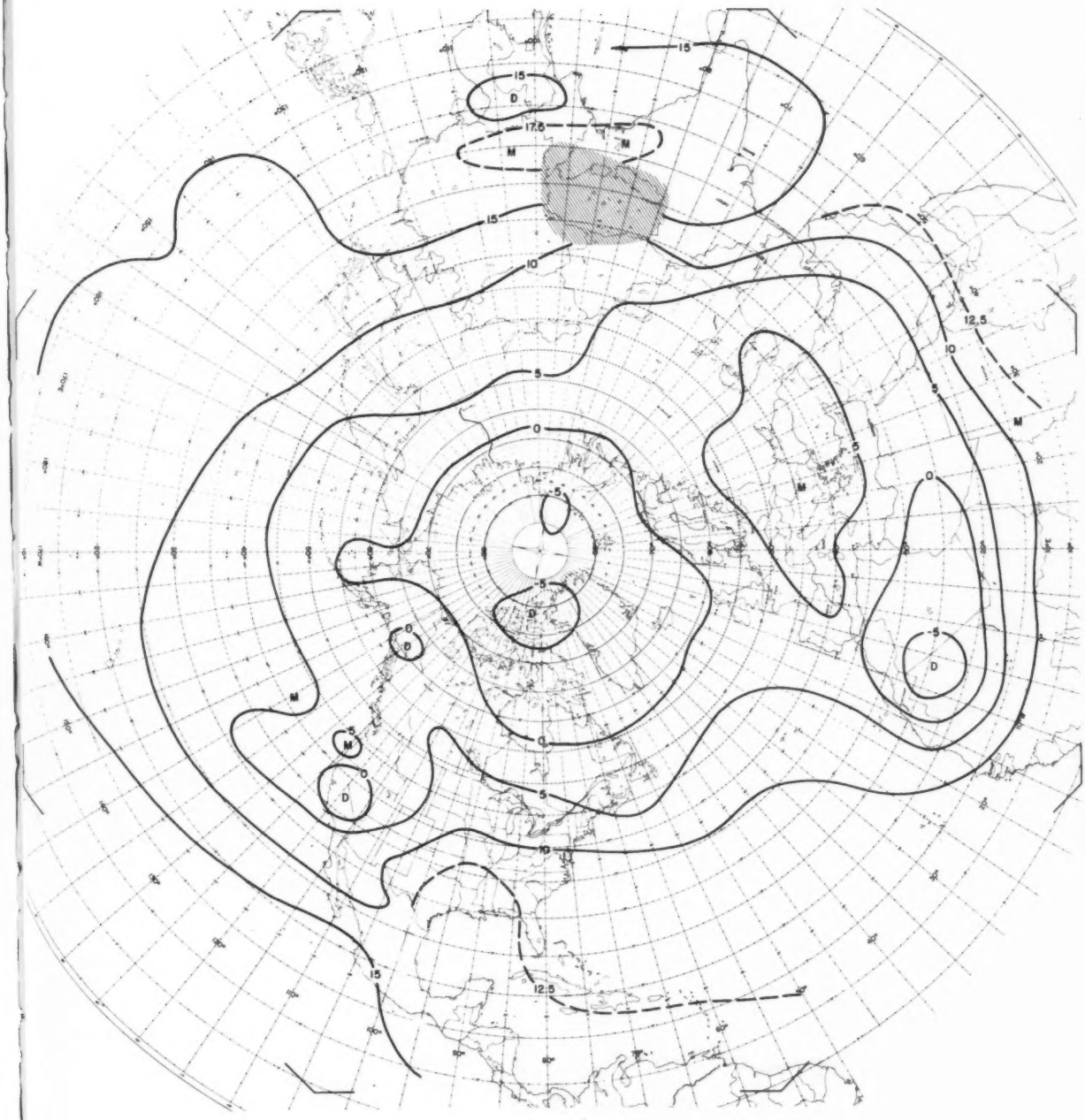

Figure 2. Plate showing dew point at 850 mb in July, 50 percentile.

prediction of *SHOCK SHAPES*

MAJOR JOHN P. THOMAS
Hypersonic Research Laboratory, ARL

Complex configurations consisting of winged and finned vehicles are anticipated in future aerospace systems. These vehicles will likely have blunted leading edges to reduce the heat-transfer problems encountered in high-speed flight. The complex shapes and blunted leading edges will cause intricate intersecting shock-wave patterns which, in turn, will produce adverse interference heating and pressure loads on a vehicle. To design these vehicles one must be able to predict the shock shapes around the body. A prediction method for shock shapes was part of an investigation done at ARL. (1)

The particular configuration studied at ARL was a basic-research shape consisting of a hemicylindrically blunted plate with a fin attached some distance downstream of the leading edge of the plate. Figure 1 shows the plate and fin shocks in relation to the model and to each other. Two additional problems, besides the intersecting shock waves, were faced with the ARL model. The shock wave of the fin was formed in a region of nonuniform Mach-number flow and interacted, as well, with the established boundary layer of the plate. The work shown here points out the comparison between the analytical and experimental shock shapes for the ARL model.

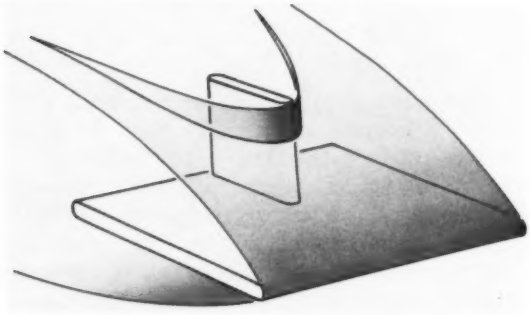

Figure 1. Fin-plate model with associated shock waves.

Looking at the blunt flat plate at a Mach number of 11.26 first, we find that the installation of the fin downstream of the plate leading edge has no measurable effect on the shock shape or location for the blunt flat plate. In Figure 2 the experimental total pressure surveys are shown for the basic flat plate with no fin attached. It may be noted that the plate had the same shock shape for angles of attack from 10-degree compression ($C10^{o}$) to 10-degree expansion ($e10^{o}$). Much greater angles of attack will produce different results; but it appears that, for small angles, the nose of the blunt plate is the controlling factor for the shape of the shock. Total-pressure surveys were made with the fin attached, and no measurable difference in shock shape was found for the three different angles. To further check on the shock shape, schlieren photographs were taken with and without the fin attached to the plate. These gave the same results as the total-pressure surveys mentioned above. Figure 2 shows the schlieren results. The vapor-screen technique was used as the final method for visualization of the shock shapes for the blunt plate. To produce the vapor screen, one operates the tunnel near the condensation limit and photographs reflected ultraviolet light from the vapor particles in the flow of the tunnel. Once again the shock shape remained quite similar. The data are depicted in Figure 2.

One comes to the conclusion that the blunt-flat-plate shock shape for small angles of attack ($\alpha = \pm 10^{o}$), regardless of whether the fin is attached or not, remains fixed within measurable accuracy. The data discussed thus far have been experimental. No mention has been made of a theoretical prediction method.

Now if one could predict the shock shape by a simple inviscid method, it would help the designer considerably. The blast-wave analogy as shown by the continuous curve of Figure 2 matches the experimental data. The analytical method is inviscid while the three different types of experimental data include effects of a boundary layer next to the plate.

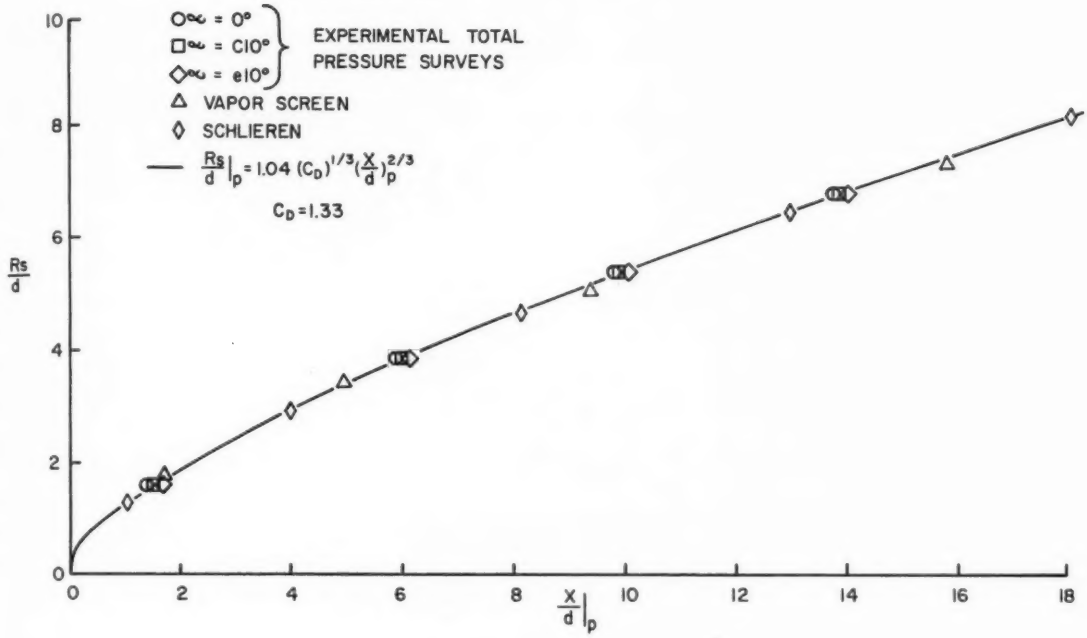

Figure 2. Blunt-plate shock shape at Mach number ≈ 11.

Reference 2 was used for the blast wave analogy. It has a shock shape equation of the form

$$\frac{R_s}{d} = K\left(C_D\right)^{1/3}\left(\frac{x}{d}\right)^{2/3},$$

where

R_s = shock radius

C_D = leading edge drag coefficient

x = axial distance on plate

d = leading edge diameter

K = coefficient, varying with Mach number.

Next let us turn our attention to the shock wave formed by the fin which is attached to the flat plate. In this case, since the flow has already passed through the blunt-plate shock, the Mach numbers approaching the leading edge of the fin vary from the plate surface to the upper tip of the fin. In fact, the blunt-plate shock intersects the leading edge of the fin approximately two thirds of the way up the fin. Besides the variation in Mach number at the fin leading edge, the blunt flat plate has an established boundary layer which has separated from the plate surface prior to reaching the leading edge of the fin. These two additional problems must be considered as disturbing influences when the shock shape of the fin is considered. An approaching Mach number of three was predicted for the fin by using the analytical method of reference (1). A program similar to that for the flat plate was undertaken for the fin, except that no facilities were available at ARL to test the fin, without the plate attached, at a Mach number of three. Therefore, experimental data were taken from NASA reports to establish the basic shock shape at a Mach number of three, as shown in Figure 3. It was not possible to use the schlieren for the fin because the light path was obliterated by the plate. The vapor-screen technique could be utilized; the results are presented in Figure 3 for the fin while attached to the flat plate.

Next, total pressure surveys were taken while the fin was attached to the blunt flat

plate. The fin was varied between an angle of 10-degree compression (C10°) and 10-degree expansion (e10°). The data from these are shown in Figure 3. The experimental results, taken from NASA reports, were for a blunt flat plate with no protuberances, while the vapor-screen and total-pressure surveys of the present work were taken with the fin attached to the flat plate. A good comparison resulted between the two experimental programs so that one might expect that the blast-wave analogy would apply here, even though the fin leading edge rests in a much more complicated flow field than the leading edge of the blunt flat plate.

One more problem should be examined at this time. The blast-wave analogy was derived for Mach numbers much greater than one, and the shock shape shows increasing error as the Mach number of the flow is reduced toward one. For the blunt flat plate, the best constant K for the shock-shape equation was found to be 1.04, and for the fin, 1.37. They are both larger than the constant in Lukasiewicz's report (2); however, his analysis was derived for the very-high-Mach-number case. The equation for the blast wave, with the constant changed, matches the experimental data at Mach numbers of 11.26 and 3.0 very well, as may be noted in the figures. The good comparison is remarkable in view of the fact that the total-pressure surveys of the fin shock shape were taken in a region completely inclosed by flow behind the blunt flat plate.

From this study one may conclude that inviscid shock shapes work very well in describing the actual conditions existing about a body in hypersonic flight. For the fin shock, the nonuniformity of the upstream Mach number, the separated boundary layer of the plate, the intersection of the plate and fin shocks, or even the fact that a boundary layer exists at all for the plate have no measurable effect on the results. These results indicate that the designer may take simple shock shapes from basic-research studies and combine them to describe the shock-shape pattern for a complicated body shape. Small angles of attack may be included in the analysis and still be correct. For further evidence that the present procedure may be applied to complicated shapes, see (1) and (3).

REFERENCES

(1) Thomas, John P., Major, "Investigation of the Pressure Distribution on a Blunt-Fin Blunt-Plate Combination at a Mach Number of 11.26," ARL 66-0142, July 1966.

(2) Lukasiewicz, J., "Hypersonic Flow-Blast Analogy," AEDC TR-61-4 (AD 259455), June 1961.

(3) Thomas, John P., Major, "The Effect of Aerodynamic Control Surfaces on High-Speed Vehicles," OAR Research Review, V, 9, November 1966.

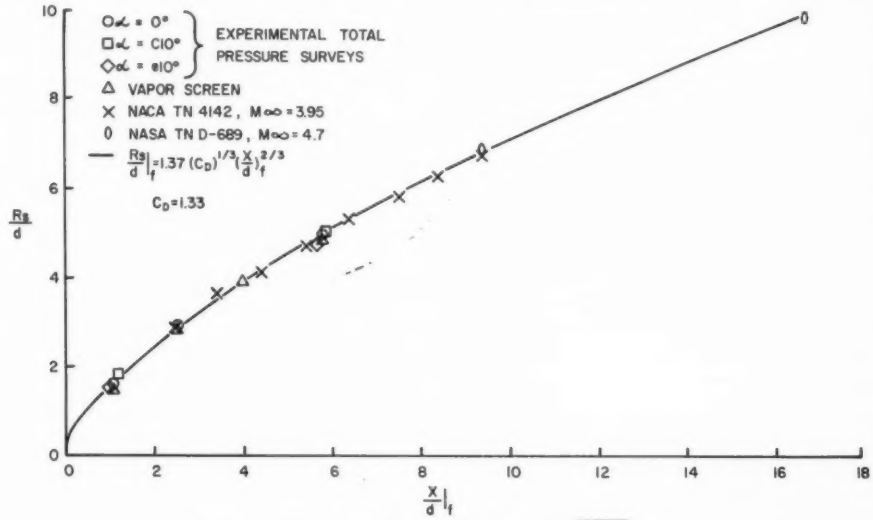

Figure 3. Fin shock shape at Mach number ≈ 3.